Constraints on hopanes and brGDGTs as pH proxies in peat

Valentine Schaaff, Vincent Grossi, Matthew Makou, Yannick Garcin, Pierre Deschamps, David Sebag, Benjamin Ngounou Ngatcha, Guillemette Ménot

Constraints on hopanes and brGDGTs as pH proxies in peat

Valentine Schaaff[1], Vincent Grossi[1], Matthew Makou[1], Yannick Garcin[2], Pierre Deschamps[2], David Sebag[3], Benjamin Ngounou Ngatcha[4], Guillemette Ménot[1]

[1] Université de Lyon, ENS Lyon, UCBL, CNRS, UMR 5276 LGL-TPE, 69364 Lyon, France
[2] Aix Marseille University, CNRS, IRD, INRAE, CEREGE, Aix-en-Provence, France
[3] IFP Energies Nouvelles, Earth Sciences and Environmental Technologies Division, 1 et 4 Avenue de Bois-Préau, 92852 Rueil-Malmaison, France
[4] Department of Earth Sciences, Faculty of Sciences, University of Ngaoundéré, Ngaoundéré, Cameroon

Corresponding author: Valentine Schaaff valentine.schaaff@ens-lyon.fr

Abstract: pH is one of the major parameters governing peat functioning, and pH variations in modern peatlands affect carbon and methane production and consumption. Paleo-pH reconstructions have been limited thus far, but they could help to better understand peat functioning in variety of settings and also serve as an indirect proxy for climatic and environmental variations such as precipitation. Bacterial hopanes and branched Glycerol Dialkyl Glycerol Tetraethers (brGDGTs) were investigated in a 10-ka peat record from North-East Cameroon (NGaoundaba, Western Central Africa). Recently developed pH proxies using the hopane ββ/(αβ+ββ) ratio and the brGDGT cyclization ratio (CBT_{peat}) were applied and compared with previously published bulk organic data from the same core. Different hypotheses are usually proposed to explain the high abundance of the "thermally mature" C_{31} αβ hopane in peats: acid-catalyzed isomerization of ββ to αβ isomers with or without biological mediation or the direct input of C_{31} αβ hopanes by bacteria. In the NGaoundaba peat deposit, the opposite variation in the ββ/(αβ+ββ) ratio of C_{30} and C_{31} hopanes and the carbon isotopic composition of C_{31} ββ and αβ hopanes suggests that an eventual transformation of C_{31} ββ to αβ isomers is not possible without biological mediation. A linear correlation between hopane- and brGDGT-reconstructed pH is observed, suggesting a similar response to environmental changes for these two independent proxies. A large increase in reconstructed pH values coincides with changes in vegetation and precipitation at the end of the African Humid Period (AHP). Lower pH values are observed during the AHP, coinciding with a period of increased precipitation and consistent with bulk organic data and slightly higher C_{31} ββ hopane $\delta^{13}C$ values compared to middle and late Holocene. Bulk organic data indicate an interruption of the AHP by a drier intermission that coincides with a decrease in reconstructed pH values, probably reflecting a decrease in evapotranspiration. Variations in pH values could be interpreted in terms of preservation of peat organic matter and might reflect past changes in methane cycling in the investigated peatland. The present study reinforces the idea that reconstruction of pH in peat deposits represents a promising proxy of environmental change, enabling a better understanding of changes in peat functioning over large timescales and various locations.

Keywords: Lipid biomarkers, hopane isomer ratios, ^{13}C composition, pH reconstruction, African Humid Period

1. Introduction

Peat deposits are important carbon sinks that are becoming increasingly important for the scientific community because they are sensitive to anthropogenic climate change (e.g., Belyea and Malmer, 2004; Leifeld and Menichetti, 2018; Loisel et al., 2021). Continental records can be scarce and discontinuous but peat deposits have great potential to improve our understanding of past climate variations, especially using proxies based on organic biomarkers (e.g., Naafs et al., 2019) due to the high content and good preservation of organic matter in peat deposits (Moore, 1989). Developing new proxies based on lipid biomarkers for paleoclimatic and paleoenvironmental reconstructions is limited by our understanding of the origin and diagenesis of these compounds in sediments (e.g., Castañeda and Schouten, 2011; Naafs et al., 2019) and by the lack of records in some areas, especially in the tropics. Recent advances in peat and biomarker proxies are expanding our ability to reconstruct past climates and environments (Naafs et al., 2019 and references therein). Several peat-calibrated proxies based on different classes of compounds, such as hopanoids and branched glycerol dialkyl glycerol tetraethers (brGDGTs) have recently been developed (Naafs et al., 2017; Inglis et al., 2018; Zhang et al., 2020), extending the possibilities of paleoclimatic reconstructions based on peat studies. Peat pH has a strong influence on microbial communities (e.g., Girkin et al., 2020), peat organic matter preservation (Moore, 1989) or methane production and consumption (Dunfield et al., 1993). Paleo pH reconstructions could constrain the evolution of peat formation and carbon/methane cycling on geological timescales. In addition, pH variations have been suggested to reflect past changes in vegetation or precipitation and paleo-pH reconstructions may therefore represent new indirect proxies of these paleoclimatic parameters.

Hopanoids are pentacyclic triterpenoids commonly found in diverse geological settings, where they generally occur as hydrocarbons (i.e., geohopanoids) (e.g., Quirk et al., 1984; Ries-Kautt and Albrecht, 1989; Innes et al., 1997; Farrimond et al., 2003). These compounds are produced by a wide range of bacteria, although estimates of the frequency of hopanoid biosynthesis among bacteria are still unclear (Rohmer et al., 1984; Pearson et al., 2007). The role of biological hopanoids is proposed to be similar to that of eukaryotic sterols, which regulate membrane fluidity and permeability (e.g., Ourisson et al., 1987), as biohopanoids have been shown to play role in bacterial outer membrane ordering (Sáenz et al., 2015). A role in protection against pathogens or pH homeostasis has also been reported (Welander et al., 2009; Schmerk et al., 2011). Hopanoids are promising biomarkers for the reconstruction of methane cycling in peats based on their carbon isotopic signature (Hayes et al., 1990; Pancost et al., 2007; Inglis et al., 2019) and their use as proxy for pH variations in peats based on specific ratios of hopane isomers has also been suggested (Huang et al., 2015; Inglis et al., 2018). Isomerization of biologically-derived 17β,21β(H)-hopanoids (hereafter abbreviated ββ) into the more thermally stable 17β,21α(H) (βα) and 17α,21β(H) (αβ) forms, as well as their isomerization at the C22 position, are well known to occur during the thermal maturation of sediments (Ensminger et al., 1974; Mackenzie et al., 1980; Mackenzie and McKenzie, 1983). Accordingly, isomer ratios have been used to describe the thermal maturity of sediments (e.g., Farrimond et al., 1996). In peat deposits, high proportions of the αβ stereoisomer have been reported despite the low thermal maturation of these sediments (e.g., Quirk et al., 1984; He et al., 2015; Huang et al., 2015; Inglis et al., 2018) and the abundance of C_{31} αβ hopanes has even been used to trace input of acidic peat into marine sediment (Smittenberg et al., 2004; Inglis et al., 2022). A direct input of αβ hopanes by indigenous bacteria could explain their high abundance (Rosa-Putra et al., 2001). It has also been suggested that these compounds are formed by microbially mediated isomerization (Ries-Kautt and Albrecht, 1989) or by acid-catalyzed isomerization without microbial mediation (Pancost et al., 2003; Inglis et al., 2018). This isomerization reaction may also be influenced by temperature and redox conditions (Huang et al., 2015), but a lack of correlation between isomerization of geohopanoids and temperature has been demonstrated in global peat database while a significant correlation with peat pH was observed (Inglis

et al., 2018). To date, the cause of the high abundance of αβ hopanes in peat is still unclear and debated.

Branched glycerol dialkyl glycerol tetraethers (brGDGTs) are prokaryotic membrane-spanning lipids. Unlike isoprenoid GDGTs produced by Archaea, brGDGTs are of bacterial origin (Weijers et al., 2006). BrGDGTs were first identified in a Dutch peat bog (Sinninghe Damsté et al., 2000) and since then, a wide range of brGDGTs with various number of methylation and cyclopentyl moieties have been found in natural environments (Schouten et al., 2000b, 2013). *Acidobacteria* have been proposed as the main producers of brGDGTs since they are abundant in soils and peats and produce isodiabolic acid, a potential building block of brGDGTs (Weijers et al., 2009; Sinninghe Damsté et al., 2011, 2014, 2018). Recent culture studies have confirmed that Acidobacteria are likely the main source of brGDGTs (e.g., Chen et al., 2022; Halamka et al., 2023), but other producers than *Acidobacteria* cannot be excluded (Weber et al., 2018). Biosynthetic pathway of brGDGTs based on the condensation of two branched dialkylglycerols instead of the reduction of tetraesters of glycerol based on isodiabolic acid has also been suggested (Weijers et al., 2006; Halamka et al., 2023). Environmental parameters exert significant control over brGDGTs distribution, with the cyclization ratio (CBT) primarily dependent on pH and the methylation ratio (MBT) primarily influenced by temperature (Weijers et al., 2007; De Jonge et al., 2014). Numerous empirical calibrations for temperature and pH have been developed over the past decades as a result of technical improvement and the need for environment-specific (lake, marine, peat, and soil) global and local calibrations (e.g., Peterse et al., 2012; Loomis et al., 2012; Naafs et al., 2017; Dearing Crampton-Flood et al., 2020; Martínez-Sosa et al., 2021).

A statistically significant correlation between brGDGT-based and hopane-based reconstructed pH values was observed in a global peat database, whereas striking similarities between the two pH reconstructions were obtained in an early Paleogene lignite deposit from Schöningen (Germany) (Inglis et al., 2018). However, applications of these pH calibrations have remained limited until now (Zhang et al., 2020). Peat brGDGT-based pH reconstructions using a previous soil calibration from Weijers et al. (2007) showed large pH variations associated with major changes in peat-forming vegetation (Weijers et al., 2011; Nichols et al., 2014) or with changes in humification associated with changes in precipitation (Zheng et al., 2015; Wang et al., 2017).

In this study, we further investigate the distribution of hopanes and brGDGTs in peat samples and their respective use as tracers of pH variations. The results are based on a 10-ka record from the NGaoundaba peat deposit located on the Adamawa Plateau (North East Cameroon, West Africa), already constrained by a study on bulk organic parameters (Schaaff et al., 2023). By comparing various parameters for hopane and brGDGT distributions (relative abundances, specific ratios, and carbon isotopic data for C_{31} hopanes), we propose new constraints on the origin of hopanes distribution in peat. The comparison of hopane- and brGDGT-based pH reconstructions further allows us to assess the applicability of these reconstructions to Holocene peat records and their potential paleoclimatic and paleoenvironmental interpretations.

2. Material and methods

2.1. Study site

The Ngaoundaba peat deposit is located in a volcanic crater on the Adamawa Plateau in Northeast Cameroon (N7.135° E13.690°, 1175 m above sea level). The vegetation at the Ngaoundaba peat deposit is dominated by sedges (*Cyperus spp*) while the site lies in the Soudano-Guinean shrubs savannas zone (Letouzey, 1958). Present day climate is characterized by two contrasting seasons: a 7-month rainy season from April to October, and a 5-month dry season from November to March. The mean annual air temperature (MAAT) is 22.2°C and the mean annual precipitation (MAP) is 1482 mm (CRU database, Harris et al., 2014). The average monthly temperature ranges from around 20.6 in December to 24.5 °C in March (CRU database, Harris et al., 2014).

2.2. Sediment core, ^{14}C dating and bulk organic analyses

A 6-meter-long core (named NGBA19) was collected in February 2019 using a Russian peat corer. The core is composed of dark brown peat without visible sandy or clayey zones. The core was then sub-sampled at 2.5-cm intervals. Organic geochemical analyses were performed on 73 samples.

The age model of the Ngaoundaba peatcore is based on 30 radiocarbon dates carried out at the LMC14 Laboratory (Saclay, France). Details on the dating and calibration of the age model are given in Schaaff et al. (2023).

Bulk organic analyses are presented in detail in Schaaff et al. (2023) To summarize, samples were analyzed for Total Organic Carbon (TOC) and $\delta^{13}C$ composition of TOC (hereafter $\delta^{13}C_{bulk}$) using an elemental analyzer (Vario ISOTOPE Select, Elementar) coupled to a thermal conductivity detector and an isotope ratio mass spectrometer (Vision, Elementar). A working standard (IVA sediment) was analyzed every 10 samples and used to normalize the mass spectrometer signals.

2.3. Organic geochemical analyses

2.3.1. Sample preparation

All samples were freeze-dried, ground and homogenized. Extraction was performed two times for 0.3g of each sample with 10mL of dichloromethane (DCM)/methanol (3:1, *v/v*) using a MARS 6 CEM microwave extraction system. Following each extraction, the supernatant was filtered through a sintered Teflon filter. Synthetic C_{46} GDGT was added to the combined extracts of each sample as an internal standard (Huguet et al., 2006). The total lipid extract was separated by column chromatography on silica gel into three fractions. The hydrocarbon fraction containing hopanes was eluted first with 8mL of hexane. A second fraction was eluted with 5mL of hexane/DCM (1:1, *v/v*). BrGDGTs were eluted in a third fraction with 10mL of DCM/methanol (1:1, *v/v*).

2.3.2. Hopane identification and analyses

Copper curls activated with hydrogen chloride (HCl) were added to the hydrocarbon fractions to remove elemental sulfur. After a first analysis using gas chromatography-flame ionization detector (GC-FID) (HP 6890A), gas chromatography-mass spectrometry (GC-MS) analyses (Agilent 6890N GC coupled to an Agilent 5975C MSD and Agilent 7890B GC coupled to an Agilent 5977B MSD) were performed for identification and quantification of the different compounds. Both GC-MS instruments provided comparable data. The GC-MS was equipped with a HP5 MS UI column (30 m x 0.25 mm, film thickness 0.25 µm). The oven temperature was programmed from 60°C (0.5 min hold) to 130°C at 20°C/min and then rises to 320°C at 4°C/min. This final temperature was held for 20 min. The carrier gas flow was constant at 1mL/min and the mass spectrometer was used at 70eV with a m/z range from 50 to 700. Hopanes were identified based on their retention time and mass spectrum. The identification of hopane isomers is consistent with published literature (Naafs et al., 2019). Semi-quantification was performed using the total ion chromatograms (TIC) by comparison with an external standard solution containing cholestane. The hopanes concentrations were normalized to TOC.

Prior to carbon isotopic measurements, the hydrocarbon fractions were separated into a saturated and an unsaturated fraction by column chromatography using silica gel impregnated with silver nitrate ($AgNO_3$, 10 % wt). Saturated fractions containing hopanes were eluted with 3 to 4 mL of *n*-heptane. Unsaturated fractions were eluted with 3 to 4 mL of ethyl acetate. Carbon isotopic compositions were measured at the LGL-TPE (Université Claude Bernard Lyon 1) using an Agilent 7890B GC coupled to an Isoprime visION Isotope Ratio Mass Spectrometer via an Isoprime GC-5 combustion interface (Elementar). The GC-IRMS was equipped with a VF-1ms (60 m x 0.25 mm, film thickness 0.25 µm). The GC-5 furnace was operated at 850 °C. An autotune and tests of stability and linearity of the signal were performed daily using the software ionOS. Stable carbon isotopic compositions (expressed as $\delta^{13}C$ values) were calibrated using a reference CO_2 gas reported to VPDB scale. Two Mix hydrocarbon B4 standards (A Schimmelmann, Indiana University) were measured every 4 to 5 samples and used to correct the $\delta^{13}C$ values. Samples were analyzed in duplicates when the quantity of samples allowed it

(see supplementary material for more details). The average standard deviation on the B4 standard is 0.37 ‰.

2.3.3. brGDGT analyses

Fractions containing brGDGTs were filtered using 0.45 µm PTFE filters. BrGDGT analyses were performed using High Performance Liquid Chromatography Mass Spectrometry (HPLC-APCI-MS, Agilent 1200) at the LGL-TPE (ENS de Lyon). Separation was achieved using two silica columns in series (ACQUITY UPLC BEH HILIC, WATERS) following the procedure of Hopmans et al. (2016) slightly modified (i.e. using hexane/isopropanol (98.2:1.8, *v/v*)). Peaks corresponding to brGDGTs were manually integrated and quantified using the peak area of C_{46}. BrGDGT concentrations were normalized to TOC. The selected *m/z* values are 743.9, 1050.2, 1048.2, 1046.2, 1036.2, 1034.2, 1032.2, 1022.2, 1020.2 and 1018.2.

2.3.4. Hopane- and brGDGT-based ratios and pH reconstructions

The degree of hopane isomerization was calculated using the ββ/(αβ+ββ) and 22S/(22S+22R) indices developed by Mackenzie et al. (1980). The ββ/(αβ+ββ) ratio was calculated for both C_{30} and C_{31} hopanes. The C_{31} αβ hopane was considered as the sum of the 22S and 22R isomers. The hopane-based pH reconstruction uses the C_{31} ββ/(αβ+ββ) index and was calculated using the following equation proposed by Inglis et al. (2018) for peats:

$$pH = 5.22 * \frac{\beta\beta}{\alpha\beta + \beta\beta} + 3.11 \; (n = 94, r^2 = 0.64, RMSE = 1.4)$$

The brGDGT-based pH reconstruction is based on the CBT_{peat} index using the following equation developed by Naafs et al. (2017) for peats:

$$CBT_{peat} = \log\left(\frac{Ib + IIa' + IIb + IIb' + IIIa'}{Ia + IIa + IIIa}\right)$$

$$pH = 2.49 * CBT_{peat} + 8.07 \text{ (n=51, } r^2\text{=0.58, RMSE=0.8)}$$

Compound structures (with numbering) are presented in Fig. S.1.

3. Results

3.1. Relative abundance and concentration of biomarkers

3.1.1. Hopanes

Diverse hopanes and hopenes were detected in the Ngaoundaba peat records. Hopanes range from C_{27} to C_{31} and are accompanied by C_{30} and C_{31} hopenes (Fig. 1). C_{31} hopanes are present in three different configurations: ββ, αβ-R and αβ-S isomers (Fig. 1). The C_{31} αβ-S hopane is present only between 8.4 ka cal BP and 6.0 ka cal BP, and its concentration ranges from 0 to 32.0 µg/g_{TOC} (Fig. 2 A). The concentration of C_{31} αβ-R hopane ranges from 0 to 44.4 µg/g_{TOC} (Fig. 2 A), reaching its highest concentration (above 10 µg/g_{TOC}) between 9.7 and 9.4 ka cal BP and between 8.5 to 7.3 ka cal BP, and its lowest (below 5.7 µg/g_{TOC}) from 5.8 ka cal BP to present. The concentration of the C_{31} ββ hopane ranges from 1.2 to 12.1 µg/g_{TOC} (Fig. 2 B) and shows similar variations as the C_{31} αβ-R hopane. Except for a brief period in the late Holocene, the C_{31} ββ hopane is less abundant than the C_{31} αβ-R isomer. C_{30} hopanes are dominated by the ββ isomers in most samples (Fig. 1). The concentration of C_{30} ββ hopane ranges from 0.1 to 3.5 µg/g_{TOC}, while the concentration of the C_{30} αβ isomer ranges from 0 to 1.8 µg/g_{TOC}. The concentration of C_{30} ββ hopane presents its maximum from the bottom of the core to 9.4 ka cal BP and from 8.1 ka cal BP to 5.8 ka cal BP (Fig. S.3).

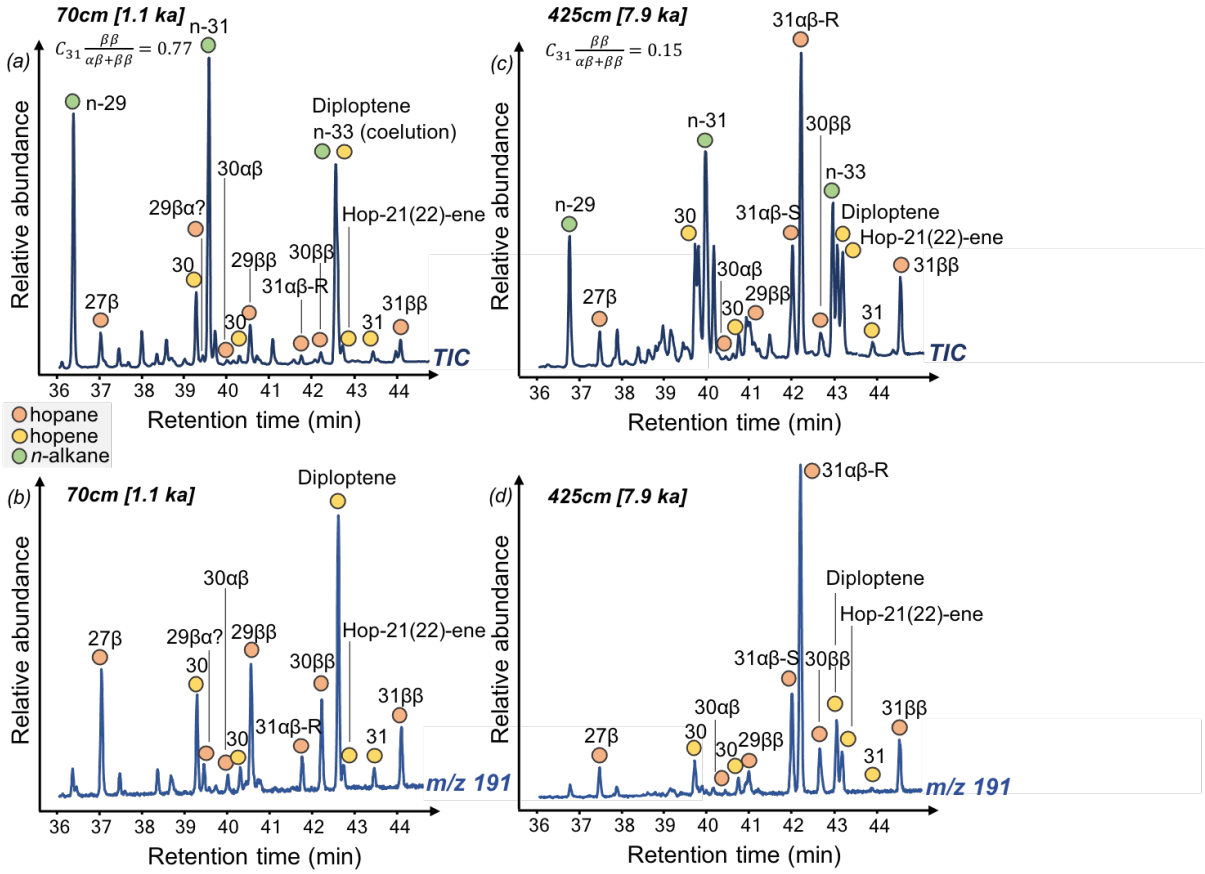

Fig. 1: GC-MS partial chromatograms of the hydrocarbon fractions of two samples with distinct hopanoid distribution: 70 cm-depth Total Ion Chromatogram (TIC) (a) and *m/z* 191 (b) and 425 cm-depth TIC (c) and *m/z* 191 (d). Ages of the samples are in ka cal BP. These chromatograms present the hydrocarbon fraction prior to separation of saturated and unsaturated compounds.

3.1.2. brGDGTs

The brGDGT assemblage is dominated by brGDGT-Ia, which represents between 57.7 and 84.6 % (see supplementary material, Table S.1 and Fig. S.2.). The concentration of the brGDGT-Ia ranges from 45.4 to 194.0 µg/g_{TOC}. The relative abundance and concentration of brGDGTs decrease with increasing number of methylation (Ia to IIIa) and degree of cyclization (Ia to Ic) (see Table S.1 and Fig. S.3 for more detail). The 6-methyl brGDGTs (IIa', IIb' and IIIa') exhibit lower relative abundances and concentrations than their 5-methyl counterparts.

3.2. Carbon isotope composition of C_{31} ββ and αβ-R hopanes

The $\delta^{13}C$ composition of the C_{31} αβ-R and C_{31} ββ hopanes could be measured for 42 and 43 out of 73 samples, respectively, most of them in duplicates. The $\delta^{13}C$ of the C_{31} αβ-R hopane ranges from around -25.8 to -18.7 ‰ with a mean standard deviation of 0.24 ‰ (min: 0, max: 0.9) (Fig. 2 C). The most ^{13}C-depleted values of the C_{31} αβ isomer are recorded between 8.1 and 5.9 ka cal BP and between 3.5 and 3.1 ka cal BP with all values but one below -23.3‰. ^{13}C-enriched values range from -18.7 to -23.4 ‰ at 9.7, 8.5 and 4.6 ka cal BP (Fig. 2 C). The $\delta^{13}C$ composition of the C_{31} ββ hopane appears slightly ^{13}C-depleted when compared to the αβ isomer, ranging from around -36.0 to -22.6 ‰ with a mean standard deviation of 0.2 ‰ (min: 0, max: 0.8) (Fig. 2 D). The $\delta^{13}C$ value of the C_{31} ββ hopane presents a global decreasing trend towards present day with periods of short increase around 8.5 ka cal BP and at 4.7 ka cal BP (Fig. 2 D). The two C_{31} hopane isomers present similar $\delta^{13}C$ values until ca. 7 ka cal BP, after which the two $\delta^{13}C$ records diverge (Fig.2 C and D).

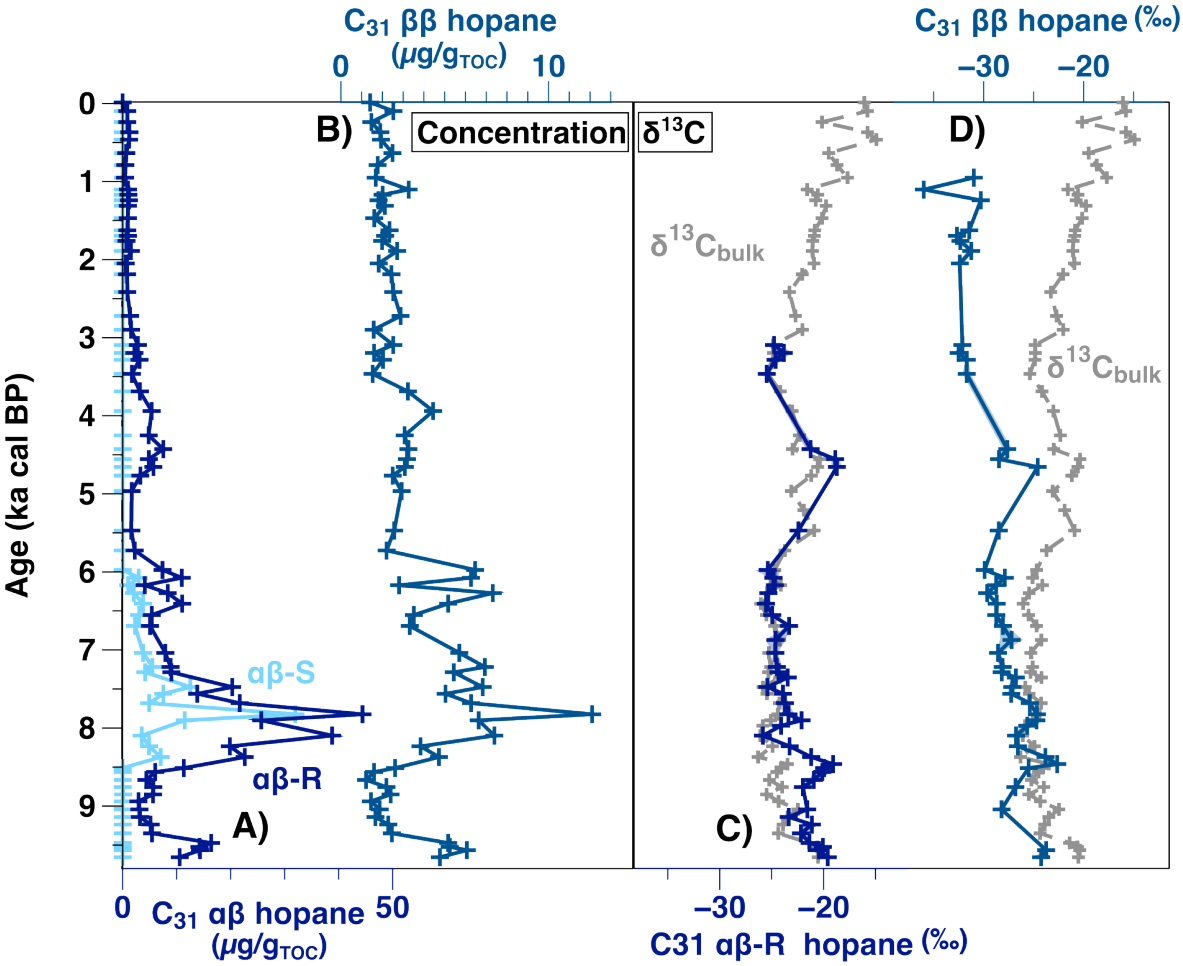

Fig. 2: Concentration of (A) C_{31} αβR and αβS and (B) ββ hopanes (μg/g_{TOC}) and carbon isotopic data for (C) C_{31} αβR and (D) ββ hopanes compared to the carbon isotopic data of bulk sediment from Schaaff et al. (2023) along the NGaoundaba peat core. The uncertainties for $\delta^{13}C_{bulk}$ values are smaller than the size of the data point, those for $\delta^{13}C_{hopane}$ values are shown on the figure but are, in most cases, smaller than the size of the data point.

3.3. Hopane stereoisomers and CBT ratios

The ββ/(αβ+ββ) indices of C_{31} and C_{30} hopanes were obtained for 67 and 49 samples out of 73, respectively. The C_{31} 22S/(22S+22R) index was only obtained for samples between 8.9 and 6 ka cal BP due to the lack of the 22S isomer in samples younger than 6 ka cal BP (Fig. S.4).

The C_{30} ββ/(αβ+ββ) index ranges from 0.4 to 0.9 (Fig. 3 A). This index is high (around 0.7-0.8) from 9.7 to 6.0 ka except for an isolated sample with a value around 0.5 at 8.8 ka cal BP. The ratio decreases to values around 0.5 between 6.0 and 5.4 ka cal BP and increases again to values around 0.7 between 5.0 and 1.0 ka cal BP. From 1.0 ka cal BP upward, the C_{30} ββ/(αβ+ββ) index shows its lowest values with minima around 0.8 ka cal BP and in the topmost sample corresponding to the post bomb period (Fig. 3 A).

The C_{31} ββ/(αβ+ββ) index ranges from 0.1 to 0.8 (Fig. 3 B). This index is low until 6.0 ka cal BP with values below 0.4 and presents its lowest values (below 0.2) between 8.5 and 7.4 ka cal BP. The ratio then increases until ca. 4.9 ka cal BP, and after a period of values below 0.5 between 4.9 and 2.8 ka cal BP, the late Holocene is characterized by values above 0.6. Short time-scale variations are recorded between 2.0 and 1.1 ka cal BP (Fig. 3 B).

The CBT_{peat} index ranges from -1.4 to -0.7 (Fig. 3 C). This index oscillates around -1 from 9.7 to 8.9 ka cal BP, and then progressively decreases to reach its lowest values between 8.4 and 7.4 ka cal BP. The CBT_{peat} index increases between 7.4 and 4.9 ka cal BP, with a short decrease centered at 6.3 ka cal BP. It then decreases from 4.9 to 4.0 ka cal BP and increases again roughly between 4.0 to 0.9 ka cal BP with short time-scale variations. The CBT_{peat} index then decreases until the present day (Fig. 3 C).

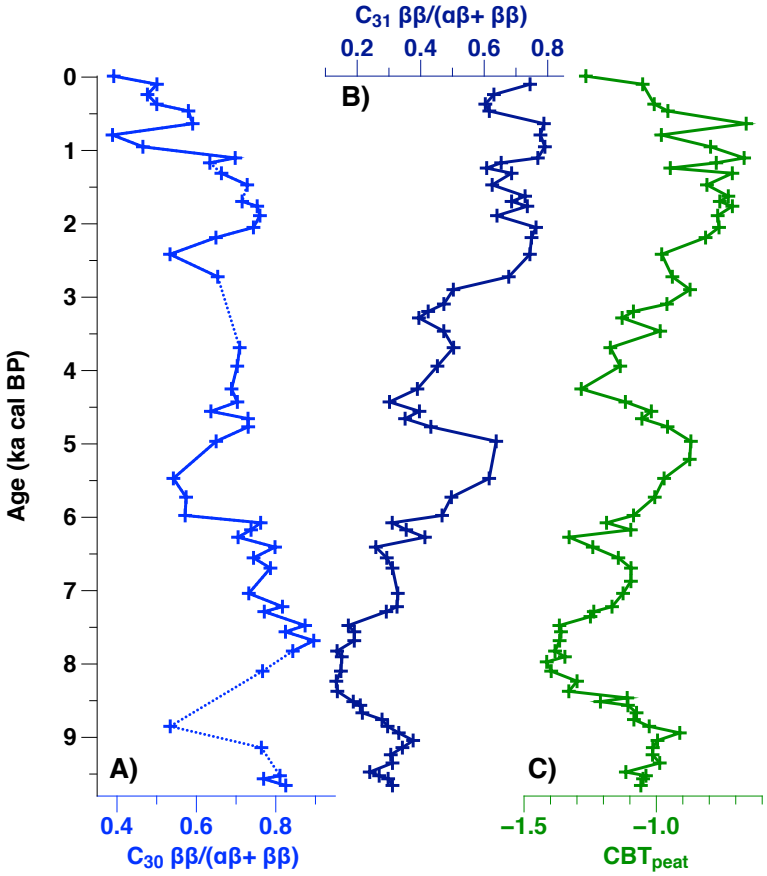

Fig. 3: Downcore evolution of hopane- and GDGT- indices with time: C_{30} ββ/(αβ+ββ) (A), C_{31} ββ/(αβ+ββ) (B) and CBT_{peat} (C). The dotted line shows the gaps in the data and the isolated values compared to the other indices.

3.4. pH reconstructions

BrGDGT-based reconstructed pH values range from 4.5 to 6.5, while hopane-based reconstructed pH values range from 3.8 to 8.3 (Fig. 4 E and F). From 9.7 to 9 ka cal BP, pH reconstructions record stable values around 4.8 and 5.5 for hopane-based and brGDGT-based reconstructions, respectively. Both pH reconstructions then decrease and present their lowest values between 8.4 and 7.4 ka cal BP. Values remain low until 6.2 ka cal BP. During the middle and late Holocene, pH globally increases with smaller scale variations visible in both pH records. In particular, both pH reconstructions show a constant decrease between 4.8 and 3.3 ka cal BP and more stable values after 3.3 ka cal BP. In contrast to the rest of the core, the shallowest samples show inverse trends for both pH reconstructions, with an increasing trend in the hopane-based pH and a decreasing trend in the GDGT-based pH (Fig. 4 E and F).

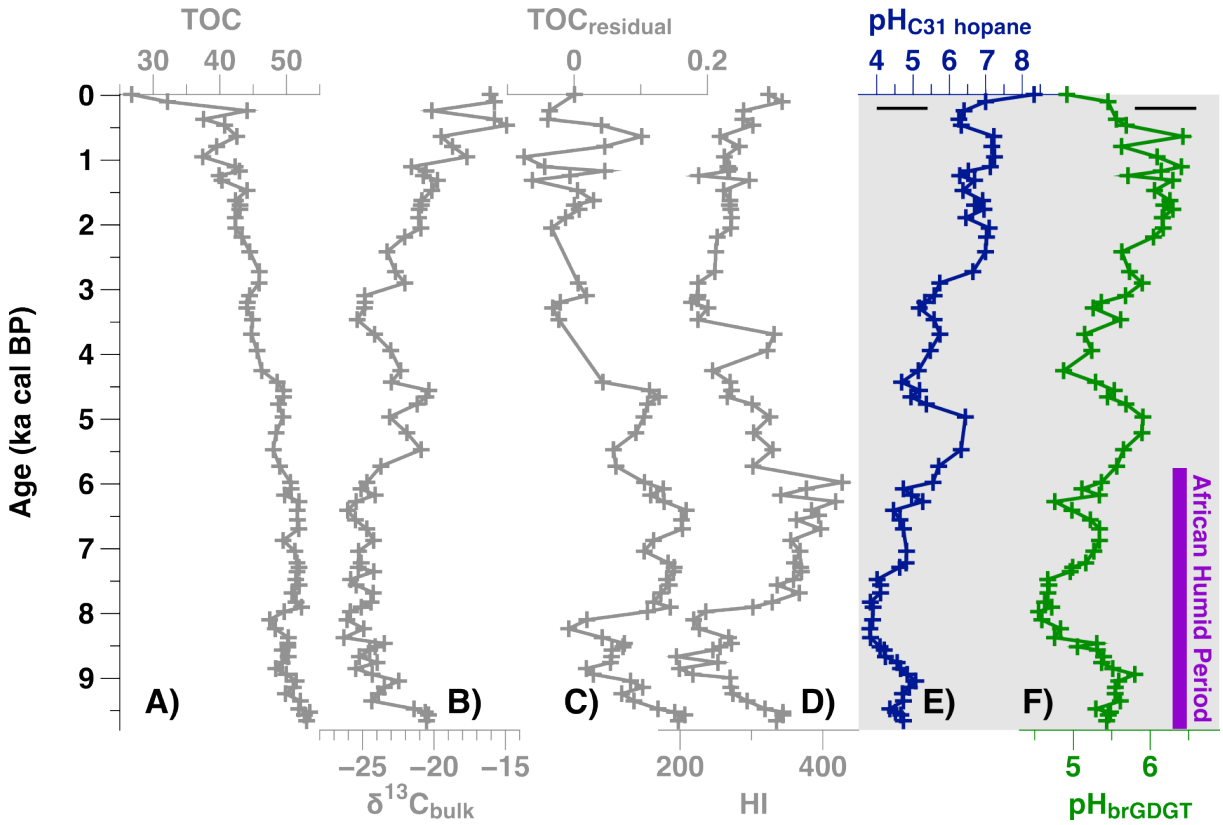

Fig. 4: Downcore evolution of bulk organic data: TOC (A), $\delta^{13}C_{bulk}$ (B), $TOC_{residual}$ (C) and HI (D) (from Schaaff et al., 2023) **and pH reconstructions: C_{31} hopane-based pH (E), brGDGT-based pH (F). The RMSE associated with each pH calibration is indicated at the top of each panel. The $TOC_{residual}$ curve was obtained by using the TOC values and a simple logarithmic decomposition model to remove the part of the signal associated with the decomposition of the organic matter (Schaaff et al., 2023). The duration of the African Humid Period at the NGaoundaba peat deposit was defined based on transitions observed in bulk organic data and is consistent with published literature (Schaaff et al., 2023).**

4. Discussion

4.1. Constraints on the origin of hopanes in peat

To explain the high abundance of C_{31} αβ isomer in peats (e.g., Quirk et al., 1984; Ries-Kautt and Albrecht, 1989; this study) as well as the correlation between the C_{31} ββ/(αβ+ββ) ratio and pH (Inglis et al., 2018), several hypotheses have been proposed and are illustrated in figure 5. Using hopanes data from the NGaoundaba peat deposit and comparison with previously published data, this section evaluates these hypotheses.

The first hypothesis proposed to explain the high abundance of the "thermally mature" αβ hopane isomers in peats characterized by low pH values relies on the abiotic isomerization of the carbon skeleton at the C17 position of the ββ isomers catalyzed by the low pH of the system (Fig. 5 A) (Pancost et al., 2003). This hypothesis is consistent with the low abundance of the C_{31} αβ hopane in peat characterized by neutral pH (Dehmer, 1995; Inglis et al., 2018) but still lacks a clear demonstration, notably from laboratory experiments. Furthermore, several observations in this study argue against such a direct acid-catalyzed isomerization of ββ hopanes. First, assuming that hopanes are produced exclusively as ββ isomers, the opposite variations in the ββ/(αβ+ββ) ratios of C_{30} and C_{31} hopanes observed throughout the core would not support a purely acid-catalyzed isomerization since C_{30} hopane and C_{31} homohopane should be affected similarly by such an abiotic process (Fig. 3 A and B and Fig. S.5). C_{30} and C_{31} hopanes are most likely produced by different sources, with C_{31} hopanes

primarily produced by heterotrophs and C_{30} hopanes possibly produced by a broader range of sources, including methanotrophs (Inglis et al., 2019). If the isomerization from ββ to αβ hopanes is acid-catalyzed, C_{30} and C_{31} ββ/(αβ+ββ) ratios should follow similar trends regardless of the initial concentration of ββ isomers produced. Second, isomerizations by intramolecular rearrangement have no or limited isotope effect (Hightower and Hall, 1967), which is consistent with C_{31} ββ and αβ hopanes having similar $\delta^{13}C$ values during early diagenesis in oil shale (Sinninghe Damsté et al., 1995). The $\delta^{13}C$ values of C_{31} ββ and αβ hopanes present similar core profiles but differ by up to 5 to 10 ‰ at both the NGaoundaba peat deposit (Fig. 2 C and D) and the Dajiuhu peatland (Huang et al., 2018, see supplementary material), arguing against a direct acid-catalyzed isomerization of hopanes sharing the same biological source organism(s). The NGaoundaba peat deposit has a significant difference of up to 10 ‰ compared to the Dajiuhu peatland (Huang et al., 2018) and the global peat database (Inglis et al., 2019), which rarely exceeds 5 ‰. The $\delta^{13}C$ values of C_{31} ββ and αβ hopanes differ mainly after ca. 7 ka cal BP (Fig. 2 C and D), suggesting a change in the microbial community after 7 ka cal BP leading to different sources of C_{31} ββ and αβ hopanes. This change in bacterial community could be driven by changes in physico-chemical conditions, such as the progressive increase in pH after 7 ka cal BP (Fig. 4 E and F).

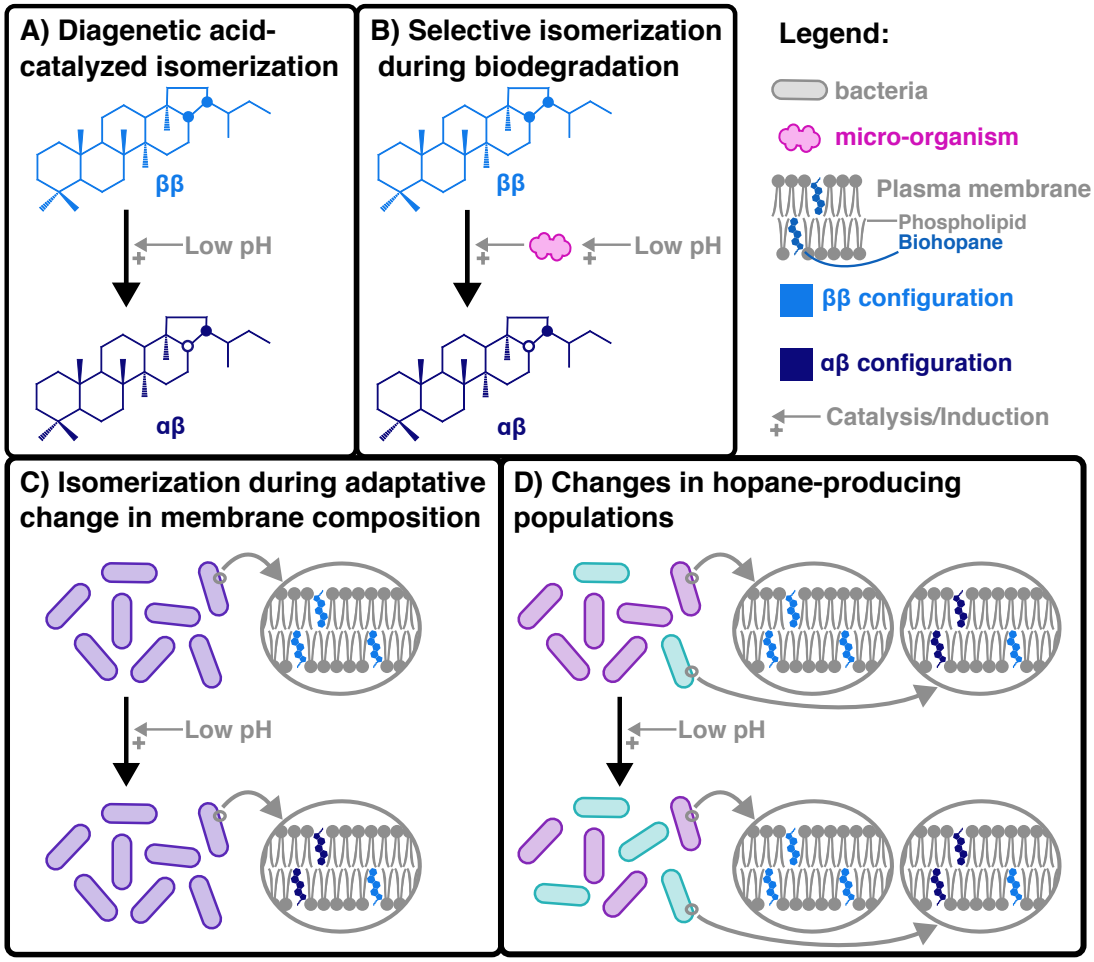

Fig. 5: Different hypotheses are proposed to explain the high concentrations of the C_{31} αβ hopane in peats and the correlation between the C_{31} ββ/(αβ+ββ) ratio and pH. (A) The biologically produced ββ is isomerized abiotically into the C_{31} αβ hopane catalyzed by the low pH of the peat. (B) The C_{31} ββ hopane is isomerized into the C_{31} αβ hopane during the biodegradation by microorganisms. The development of the microorganisms involved in this degradation is likely pH-sensitive. (C) Both ββ and αβ configurations are biologically produced. Changes in membrane composition occur as an adaptation to changing pH. (D) Both ββ and αβ configurations are biologically produced and each

species of bacteria has its own biohopane composition. Changes in the microbial community in response to pH variations are responsible for the observed distribution of ββ and αβ geohopanes. For simplification, bacterial membranes are represented here as a simple bilayer composed of phospholipids and biohopanes.

Such findings point to either a biological transformation of ββ hopanes into αβ isomers during biotransformation (Fig. 5 B) (Ries-Kautt and Albrecht, 1989), or a direct bacterial input of hopanes, with different isomeric configurations (Fig. 5 C or D). Hopanes has been shown to undergo selective biodegradation, such as during the demethylation at C25 of hopanes, which occurs preferentially in low molecular-weight hopanes and favors different epimers (22S and 22R) depending on molecular weight (Requejo and Halpern, 1989; Peters et al., 1996). Hopanes with different shapes, dimensions and volumes, as well as different molecular weight and isomerization may affect their biodegradation (Peters et al., 1996), but more research is needed to estimates these effects in sediment of low thermal maturity. The different evolution of C_{30} and C_{31} ββ/(αβ+ββ) hopanes ratios could be attributed to selective biodegradation. It has been shown that some bacteria are capable of producing biohopanoids epimers at C-22 (Peiseler and Rohmer, 1992) or ββ, βα and αβ biohopanoids although this has only been demonstrated in only one strain of Frankia sp. so far (Rosa-Putra et al., 2001). On the other hand, bacteria are able to alter their membrane composition in response to changes in environmental parameters, enabling them to maintain acceptable membrane fluidity and cell activity (Fig. 5 C) (e.g., Russell and Fukunaga, 1990; Vinçon-Laugier et al., 2017). Changes in microbial community structure as well as membrane lipid composition are used to explain the observed changes in MBT and CBT indices and in temperature and pH calibrations based on brGDGTs (e.g., Weijers et al., 2007; Huguet et al., 2014; De Jonge et al., 2021; Naafs et al., 2021; Halamka et al., 2023). A similar adaptation may exist in biohopanoid-producing bacteria, with greater production of the more stable αβ-isomers under more acidic conditions (Fig. 5 C). However, as far as we know, the impact of pH variations on the biohopanoid composition of bacterial membranes is not known and functionalized biohopanoids with the αβ configuration have only been reported in Frankia spp (Rosa-Putra et al., 2001). Further studies showing the occurrence of αβ hopanoids in living organisms are clearly needed. In addition, very few data are currently available on the steoreochemistry of biohopanoids such as bacteriohopanepolyols (BHPs) in modern peat samples (e.g., Talbot et al., 2016) which could provide an indirect evidence of the origin of αβ hopanoids.

Carbon isotopic data of microbial-derived biomarkers provide unique information about the origin of these compounds (e.g., Schouten et al., 2000a; Pancost et al., 2003; Schwartz-Narbonne et al., 2023). Overall, the range of $\delta^{13}C$ values of C_{31} ββ and αβ hopanes in the NGaoundaba peat deposit (Fig. 2 C and D) is consistent with values reported in other studies (e.g., Pancost et al., 2003; Xie et al., 2004; McClymont et al., 2008; Huang et al., 2018; Inglis et al., 2019). The $\delta^{13}C$ values of C_{31} ββ and αβ hopanes follow similar variation as the $\delta^{13}C_{bulk}$, in line with previous studies suggesting a heterotrophic origin for these compounds without a major input from methanotrophic bacteria (Pancost et al., 2003; Inglis et al., 2019). The $\delta^{13}C$ values of C_{31} αβ hopane are nearly identical to those from the C_{bulk} at the bottom of the core and from 8.1 to 6.0 ka cal BP but present a positive shift compared to the $\delta^{13}C_{bulk}$ from 9.3 to 8.2 ka cal BP. As suggested by Pancost and Damsté (2003), this shift towards higher values may suggest preferential bacterial consumption of labile ^{13}C-enriched carbon during this period. However, C_{31} ββ hopane appears to be between 0.9 and 9.6 ‰ more depleted in ^{13}C than the C_{31} αβ isomer all along the core (Fig. 2 D). Consumption of refractory ^{12}C-enriched carbon or depleted carbon sources such as methane by the producer(s) of the ββ isomer cannot be excluded. Data from the Dajiuhu peatland (Huang et al., 2018, see supplementary material) also show more depleted $\delta^{13}C$ values for C_{31} ββ hopane compared with those from C_{31} αβR hopane. The difference between the $\delta^{13}C$ values of C_{31} ββ and αβ hopanes thus supports distinct producers of these two hopane isomers that use different carbon sources (Fig. 5 D). Similarly, a source decoupling between C_{30} and C_{31} hopanes, as proposed by Inglis et al. (2019), may explain the opposite variations observed for the two hopane ratios at the NGaoundaba peat deposit (Fig. 3).

Microbial biodegradation has been shown to have diverse effect on the carbon isotopic fractionation of different lipids possibly associated with difference in the degradation pathway (Sun et al., 2004). The differences between the carbon isotopic values of the ββ and αβ isomers of hopanes might be explained by heavy isotope effects in enzyme-catalyzed reactions (Heipieper et al., 2004; O'Leary, 1980), such as those involved during biodegradation of organic matter (Fig. 5 B). In enzyme-catalyzed reactions, the magnitude of the isotope effect depends on the structure of the transitional state related to the change in bonding to the isotopic atom (O'Leary, 1980). No estimation of the isotope effect exists for hopane isomerization at present. However, a higher rate of isomerization from ββ to αβ may be expected to drive heavier ββ hopane $\delta^{13}C$ than that of αβ hopane. This has been observed for other reactions and compounds (Heipieper et al., 2004; Pan et al., 2014). At the NGaoundaba peat deposit, low values of the C_{31} hopane ββ/(αβ+ββ) ratio correlate with a period of more negative $\delta^{13}C$ values of αβ hopane, reducing the difference between αβ and ββ hopane $\delta^{13}C$ values (Fig. 2 C and D and Fig. S.9). Thus, each scenario (B), (C) and (D) is not exclusive, and a combination of several of these scenarios is possible.

4.2. Biomarker-based pH reconstructions

4.2.1. Comparison between hopane- and brGDGT-based pH reconstructions

Using the brGDGT and hopane molecular data, we reconstructed two pH records using previously published empirical calibrations (Naafs et al., 2017; Inglis et al., 2018). The two calibrations are respectively based on the C_{31} hopane ββ/(αβ+ββ) ratio and on the brGDGT CBT_{peat} ratio. These two ratios are a priori independent as they are based on two distinct classes of molecules known so far to be produced by at least somewhat different populations of bacteria.

A statistically significant positive correlation between the two pH reconstructions (r^2= 0.678, n=66, p-value<<0.01) is observed for the NGaoundaba peat record (Fig. 6 A), with only one outlier data point corresponding to the uppermost sample (at 10 cm). The latter can be attributed to different production or degradation depths between hopanes and brGDGTs. Consistent with this hypothesis, either one or both of the hopane isomers are absent from several surface peat sediments (see supplementary material in Inglis et al., 2018). In the NGaoundaba peat record, the C_{31} αβ hopanes are absent in the topmost sample, leading to a ββ/(αβ+ββ) ratio equal to 1. Consequently, a maximum pH value is obtained with the calibration from Inglis et al. (2018). Similarly, brGDGTs also show strong variations in the more recent samples, with the topmost sample having the lowest concentrations in all brGDGTs studied. The correlation between the two pH proxies suggests a similar response of these two independent proxies to environmental changes and thus supports their use for paleo-pH reconstructions despite different absolute reconstructed pH values. The range of pH values is larger for hopane-based pH than for brGDGT-based pH and therefore the correlation between the two pH reconstruction deviates from a 1:1 line (Fig. 4 E, F and Fig. 6 A).

As for the NGaoundaba peat deposit, similar variations between hopane-based and brGDGTs-based pH reconstructions were previously observed in the Schöningen lignite dating from early Paleogene (~55 Ma) (Inglis et al., 2015, 2018). We thus compared our results with those from the Schöningen lignite (Inglis et al., 2015, 2018) (Fig 6 A and B, respectively). The correlation between the two sets of pH values appears weaker for the lignite than that found for the NGaoundaba peat deposit. While the pH range reconstructed using brGDGTs is very narrow (less than 0.6 pH unit), the pH range reconstructed using C_{31} hopane isomers is much larger (around 2.6 pH unit), resulting in a correlation that strongly deviates from the 1:1 line. Because the Schöningen lignite samples are older than the NGaoundaba peat deposit samples, this result could suggest a diagenetic influence on hopane-based pH reconstruction, with an increased deviation from the 1 :1 line with time. To test this hypothesis on the hopane-based reconstructed pH values from the NGaoundaba peat deposit, we calculated the shortest distance to the 1:1 line for each data point. The absence of correlation between this distance and the sample age (Fig. S.6) indicates that the deviation from the 1:1 line is unrelated to the age of

the sample, at least for the time period covered in the present peat (ca. 10 ka cal BP) (Fig. S.6) and that diagenesis is likely not responsible for this deviation.

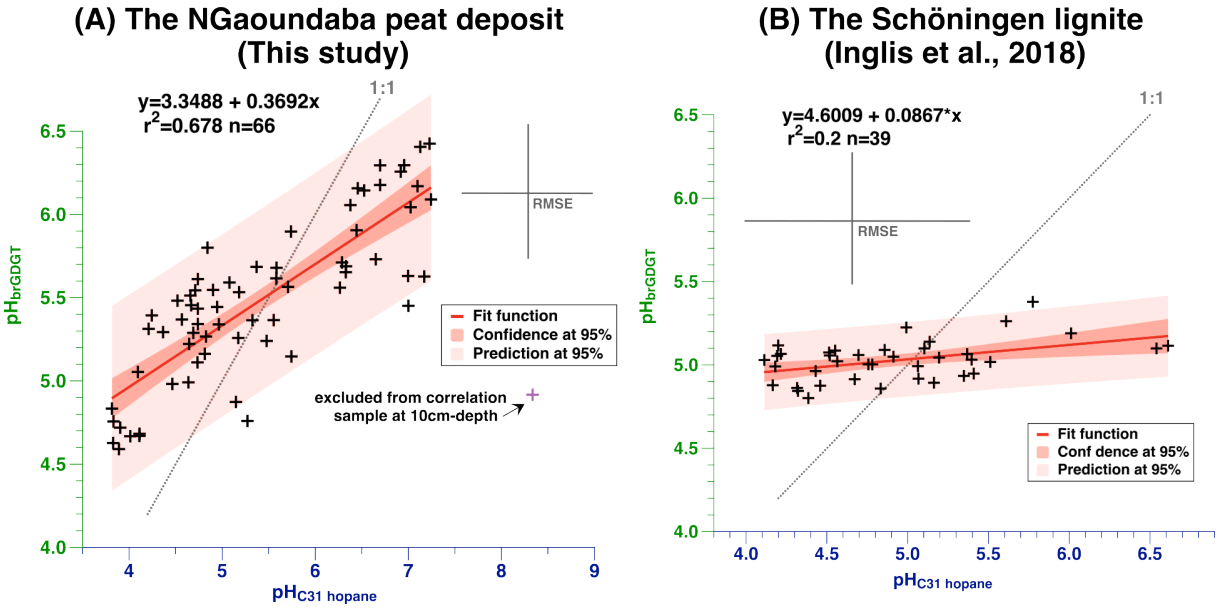

Fig. 6: Correlation between C_{31} hopane- and brGDGT-reconstructed pH values for the NGaoundaba peat deposit (This study) (A) and for the Schöningen lignite (Inglis et al., 2015, 2018) (B). The dotted line represents the 1:1 line. The RMSE associated with each pH calibration is represented in light grey. For the NGaoundaba peat deposit, the uppermost sample (10cm-depth) has been excluded from the correlation.

4.2.2. Bias in absolute pH values due to existing calibration datasets

Unlike temperature, which can be estimated using climatic models, the pH values used in empirical calibrations must be measured directly *in situ*. Such data are lacking for some sites in the global peat database, resulting in a restricted pH calibration database (51 sites for pH out of the 96 used for temperature) (Fig. 7 - Green cross) (Naafs et al., 2017). Several studies have pointed out the lack of studies based on organic compounds in tropical peatlands and its impact on our understanding of brGDGT distributions and temperature/pH empirical calibrations (Weijers et al., 2011; Naafs et al., 2017). Among low latitude sites, African sites are particularly scarce in previous calibrations, with only 1 out of 51 sites for the brGDGT pH calibration and none out of 94 sites for the hopane pH calibration (Naafs et al., 2017; Inglis et al., 2018). This poor representation of low latitude peat deposits may significantly bias the global empirical calibrations as the specificities of these low-latitude records, such as precipitation regime (amount and seasonality), vegetation types, and temperature variations are not taken into account. Vegetation types influence peat microbial activity in both temperate and tropical peatlands (e.g., Fisk et al., 2003; Andersen et al., 2013; Girkin et al., 2020). For both hopane and brGDGT pH calibrations, vegetation diversity is well represented among the sampled peats (Naafs et al., 2017; Inglis et al., 2018), meaning that biases associated with differences in vegetation (Liang et al., 2019) are likely included in calibration errors. However, in the hopane-based pH calibration proposed by Inglis et al. (2018), 63 data points out of 94 come from four Chinese peats (Fig. 7 - Blue Circles). The over-representation of the four sites located in a restricted geographical area may bias the global pH calibration and could partly explain the larger range of pH values reconstructed using hopanes compared to brGDGTs (see Huang *et al.* (2015) for details on the environmental and climatic characteristics of these four sites).

Naafs et al. (2017) demonstrated that, in general, the overall brGDGT distribution is not significantly different between the upper 15 cm (acrotelm, likely oxic) and the peat sediment underneath (catotelm, likely anoxic), but that some high-latitude peatlands show strong differences in brGDGT distribution

between both layers, likely associated with the seasonal bias of brGDGT production (Naafs et al., 2017). To address this problem, Naafs et al. (2017) retained all data from the upper 1 m without differentiating the acrotelm and the catotelm, and averaged all samples for each peatland, except for high latitude peats, where the top 20 cm were excluded. The same problem may be encountered with hopanes. While some studies show strong variations in hopane distributions (Huang et al., 2015) and concentrations (Farrimond and Flanagan, 1996; He et al., 2015) within the first meter of peat deposits, a rapid isomerization is suggested in several studies (Inglis et al., 2018; Quirk et al., 1984). The use of both surface and averaged samples from the upper first meter could therefore bias the calibrations and explain the differences between the ranges of pH values obtained from hopane and brGDGT calibrations.

The CBT_{peat} and C_{31} ββ/(αβ+ββ) values obtained for the first meter of the NGaoundaba peat deposit, along with the pH measured in the peat, were compared with the Global Peat Database, which was used to calibrate brGDGT- and hopane-based pH reconstructions (Fig. S.7). Despite the scarcity of African peat deposits in the global calibration dataset, values from the NGaoundaba site are consistent with the global calibrations, allowing interpretations derived from brGDGT and hopane distributions, as well as the carbon isotopic composition of hopanes in our study site to be generalized to other peat deposits worldwide.

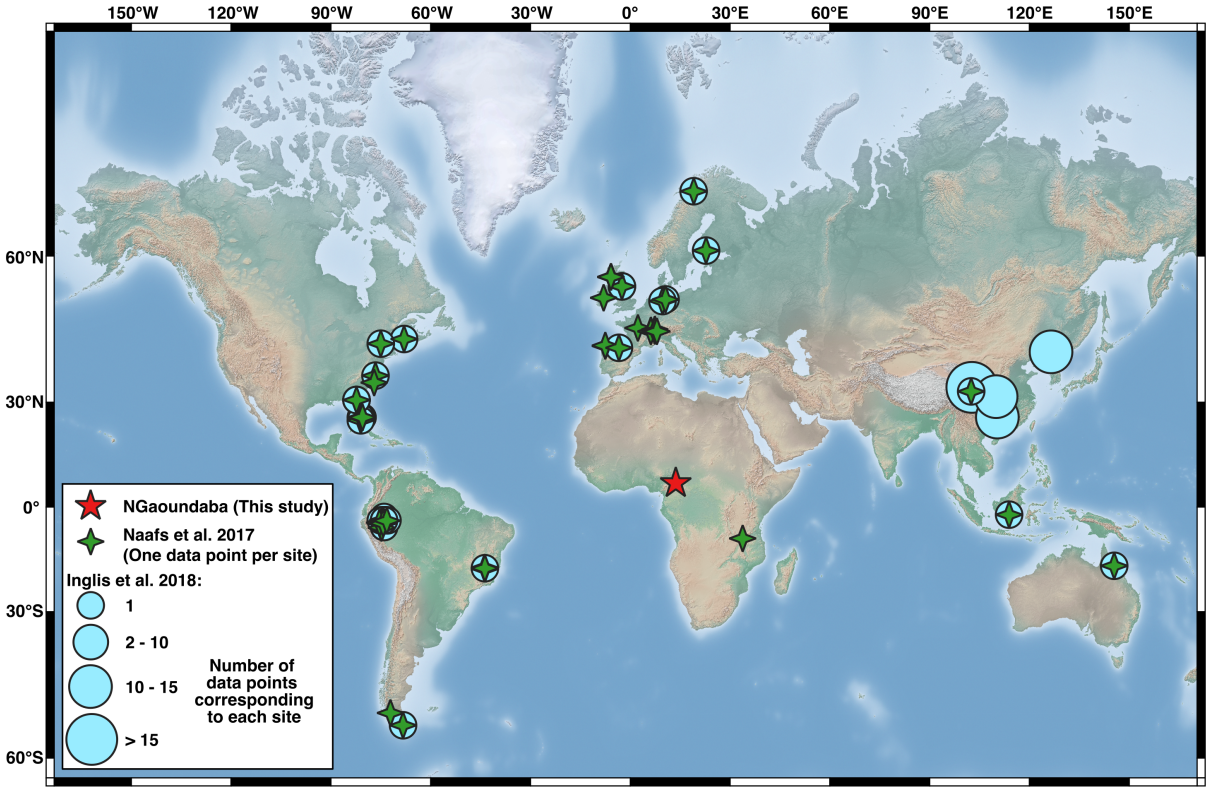

Fig. 7: Map with the location of all peats used for global pH calibrations by Naafs et al. (2017) (green cross) and Inglis et al. (2018) (blue circles). The size of the blue circles is proportional to the number of data points for each site used in the calibration. The location of the NGaoundaba peat deposit is indicated by the red star.

4.3. Local bias affecting pH reconstructions

4.3.1. Influence of microbial activity in lower peat layers

The microbial community structure has been shown to vary significantly over the first meter of peat, due to significant changes in peat properties and environmental variables such as pH, redox conditions, moisture content, or nutrient availability (e.g., Williams and Crawford, 1983; Ausec et al., 2009;

Jackson et al., 2009; Andersen et al., 2013; Too et al., 2018; Girkin et al., 2020). The upper oxic layer (acrotelm) has a relatively high decomposition rate of organic matter compared to the lower anoxic layer (catotelm) (Clymo, 1984). The upper oxic layer is dominated by aerobic decomposition mediated by fungal and/or bacterial populations (Winsborough and Basiliko, 2010; Tripathi et al., 2016). Microbial diversity and activity are highest at the surface (Jackson et al., 2009; Too et al., 2018), but a high relative abundance of certain phyla such as *Acidobacteria* has been reported in deeper layers (i.e., around 45cm-depth) (Too et al., 2018) and microbial activity has also been reported in deep (2m depth) peat horizons (Kluber et al., 2020). As *Acidobacteria* are producers of both hopanes (Welander et al., 2010) and brGDGTs (Sinninghe Damsté et al., 2014, 2011; Chen et al., 2022; Halamka et al., 2023), the potential influence of the presence of this phylum in the lower peat layer on pH reconstructions should be considered. Although brGDGTs have mostly been associated with aerobic phyla so far (e.g., Sinninghe Damsté et al., 2018), brGDGT production may require low oxygen availability (Halamka et al., 2021) and the occurrence of anaerobic producers cannot be excluded. Lipid production in the lower peat layers may cause an offset between the molecular signal and the age of the bulk peat sediment. The latter may be older than the compounds considered for pH reconstruction.

To test this hypothesis, we artificially added a positive or negative offset in one of the two pH reconstructions and recalculated the correlation between the two pH reconstructions. Specifically, $pH_{C31\ hopane}$ at time t_n was compared to the pH_{brGDGT} at time t_{n+1} with n the sample number increasing with depth, and vice versa. Adding an offset did not improve the correlation, suggesting that there is no offset between the two pH reconstructions (see supplementary material, Fig. S.8 A and B). Compound-specific ^{14}C dating, as proposed by Pancost et al. (2000), could confirm the limited impact of microbial activity in deeper layers, and provides a better understanding of microbial activity in deep peat layers. Another possibility to identify an offset is to compare the pH reconstructions with other non-microbial proxies. Major climate transitions affect both vegetation and microbial communities. In the NGaoundaba peat record, the end of the African Humid Period (AHP) is well marked in bulk organic parameters (HI, $TOC_{residual}$ and $\delta^{13}C_{bulk}$; Schaaff et al. (2023)) around 5.8 and 5.7 ka cal BP (Fig. 4 B, C and D, Schaaff et al., (2023)). A transition from low pH values during the AHP to higher pH values during the middle and late Holocene as well as changes in hopane and brGDGT concentrations are recorded between 6.0 and 5.8 ka cal BP (Fig. 4 E and F). A limited impact of the difference in response time to climate change between the microbial community and vegetation is expected (e.g., Webb, 1986; Hughen et al., 2004; Waldrop and Firestone, 2006). Thus, an offset of less than 0.3 ka cal BP may occur at the NGaoundaba peat deposit between the age model and the variations recorded in vegetation-based proxies and the variations recorded in the microbially-based proxies. The pH signal may also be an integrated signal of compounds produced in a centimetric or even decametric depth range. Weijers et al. (2011) showed an absence of correspondence between CBT-based pH values and *in situ* measured pore water pH, further suggesting that the brGDGT signal is more likely to represent a preserved 'fossil' biosignature than an *in situ* production in deep peat.

Caution is needed, however, when interpreting results from the upper part of the peat deposits. Analyses of short recent peat sequences can lead to misinterpretations, corresponding to recent changes in microbial community structure rather than to a paleoclimatic signal.

4.3.2. A seasonal bias for pH reconstruction?

Seasonality is a significant bias in brGDGT temperature reconstructions in various settings, most likely due to bacterial membrane adaptation to environmental changes or changes in the microbial community structure (e.g., Sun et al., 2011; Loomis et al., 2014; Cao et al., 2018; Miller et al., 2018). Except for seasonally frozen sites, temperature seasonality has been shown to have little impact on brGDGT temperature calibration in peats (Dearing Crampton-Flood et al., 2020; Naafs et al., 2017). While temperature seasonality is a major concern in high-latitude and temperate records, tropical regions have narrower temperature variations throughout the year, making tropical peat records less susceptible to affect temperature seasonality bias (Loomis et al., 2012; Pérez-Angel et al., 2020). However, as aforementioned, precipitation can have an impact on pH values. Because of the strong seasonal variations in precipitation that occurs in the tropics, this could affect the microbial community structure and activity, and, in turn, severely bias pH reconstructions. Marwanto et al. (2018), for example, show that drought and rewetting events affected the pH values of two tropical peatlands in Indonesia. During a drought event, the pH at 50 cm-depth decreases due to increased oxidative conditions but remains low long after the next rewetting event begins (Marwanto et al., 2018). It is beyond the scope of this study to determine how seasonal climate and environmental changes will affect pH reconstructions in peat, but additional research is undoubtedly required. Differences in sensitivity to seasonal sensitivity between brGDGT producers and hopane producers may explain, in part, the observed difference in the range of reconstructed pH values (Fig. 4 E and F and Fig. 6).

4.4. A multi-causal interpretation of pH reconstructions

Changes in reconstructed pH have been proposed to reflect past changes in precipitation, with increased precipitation leading to a dilution effect and an increase in pH (Pancost et al., 2003; Inglis et al., 2018). The minimum reconstructed pH values for the NGaoundaba peat deposit, between 8.4 and 6.2 ka cal BP, coincide with a period of increased precipitation in agreement with the timing of the African Humid Period (Fig. 4 B, C and D, Schaaff et al., (2023)) and are therefore not consistent with a potential dilution effect. Consistently, higher brGDGT-reconstructed pH values were recorded in a “dry” site compared to a “wet” site from the Frasne peatland (Jura Mountains, France), suggesting an influence of peat moisture level or oxygen availability on brGDGT distribution (Huguet et al., 2010). In paleorecords, similar relationship between peat moisture and/or precipitation and CBT-based pH (soil calibration) have been suggested (Zheng et al., 2015; Wang et al., 2017). The low pH recorded at the NGaoundaba peat deposit is also consistent with ombrotrophic conditions (wetland hydrology mostly controlled by precipitation) as opposed to minerotrophic conditions (wetland hydrology modulated by precipitation and groundwater input) which usually present higher pH (e.g., Swanson and Grigal, 1991). Two other parameters seem to strongly influence pH variations and can be responsible of pH variations in paleorecords. First, catchment lithology may have a strong impact on long term variations of peat pH. More specifically, the presence of carbonate in the catchment area and its leaching can induce alkaline input into the peatland. Among the paleopH records explored here (Zheng et al., 2015; Wang et al., 2017; Zhang et al., 2020, this study), the Dajiuhu peat deposit is the only site situated in a carbonate-dominated catchment (Zhang et al., 2022). Interestingly, this site records a decrease in hopane-based pH during the dry deglaciation period (Zhang et al., 2020) while other sites record an increase in reconstructed pH during drier periods. This suggests that the decrease in precipitation during the deglaciation at the Dajiuhu peatland decreased the runoff from the catchment and the input of alkali resulting from carbonate alteration, reducing the buffering effect of carbonate at this site.
Second, changes in the peat-forming vegetation influence peat pH since some plants, such as *Sphagnum* mosses, directly contribute to peat acidification through cation exchange (Clymo, 1963). Major transitions previously observed in CBT-based pH reconstructions were attributed to major changes in vegetation, with the transition from sedge-dominated peat to Sphagnum-dominated peat associated with lower pH values during Sphagnum-dominated interval (Nichols et al., 2014; Weijers et al., 2011). Weijers et al. (2011) associated these changes with changes in the trophic status of the peat from a fen system to an ombrotrophic bog. As the catchment area of the NGaoundaba peat deposit is

small and located in a maar crater with a slightly higher elevation than the surrounding area, this deposit has probably remained an ombrotrophic peat over the last 10 ka, fed primarily by rainfall water without a permanent water inlet. Despite the absence of Sphagnum mosses at NGaoundaba, pH variations based on brGDGTs and hopanes may coincide with major changes in local vegetation, as suggested by significant variations in $\delta^{13}C_{bulk}$ (Fig. 4 D, E and F). Such vegetation changes observed at the NGaoundaba peat deposit may coincide with changes in precipitation and associated changes such as water table depth and oxygenation level. Therefore, in the absence of *Sphagnum* mosses, simultaneous changes in vegetation and pH may only reflect a correlation between these two parameters without any causal effect.

The interpretation of past pH variations based on organic proxies remains complex, and pH variations cannot be attributed to a single cause. Prior to any interpretation in terms of change in precipitation and precipitation/evaporation balance, a good understanding of catchment characteristics (size, lithology, vegetation, and trophic status of the peat) and their evolution through time is fundamental. At the NGaoundaba peat deposit, a decrease of reconstructed pH is recorded from 9.7 to 5.8 ka cal BP which coincides with the African Humid Period. It is likely that paleo-pH reconstructions based on microbial compounds produced in-situ are also affected by changes in peat moisture level, reflecting the balance between precipitation and evapotranspiration. The progressive decrease of pH between 8.9 and 8.0 ka cal BP coincides with a period of low $TOC_{residual}$ and HI values interpreted as a potential drier intermission during the AHP (Schaaff et al., 2023). During this period, a change in evapotranspiration or in the seasonality of precipitation rather than in the amount of precipitation could explain the discrepancy between low reconstructed pH suggesting more precipitation, and low TOC and HI values suggesting a drier period (Fig. 4). Between 8.0 and 5.8 ka cal BP, reconstructed pH values present their lowest values consistent with increase precipitation interpreted based on bulk organic data (Fig 4.). Low pH values during the African Humid Period are consistent with good preservation of organic matter (Moore, 1989) and coincide with high $TOC_{residual}$ and HI values that may be associated with better preservation of peat organic matter (Schaaff et al., 2023). The increase in pH recorded in the mid- and late Holocene probably led to an increase in methanotrophy and possibly in methanogenesis (Dunfield et al., 1993) which is consistent with previous studies suggesting more methanogenesis at neutral pH values (Inglis et al., 2019).

Conclusions and perspectives

Through the joint investigation of bacterial hopanes and brGDGTs in a sequence of African peat, our study validates the use of these families of molecules for the reconstruction of pH variations but also highlights their limitations and perspectives for improvement. The comparison of C_{30} and C_{31} ββ/(αβ+ββ) hopane ratios as well as the carbon isotopic composition of C_{31} ββ and αβ isomers demonstrate that the direct acid-catalyzed isomerization of ββ into αβ isomers is unlikely without biological mediation. The influence of deep peat hopane and brGDGT production appears to be limited at the NGaoundaba peat deposit since no downcore trend in hopane and brGDGT concentrations and abundances is observed and limited offset with proxies independent of microbial production has been found. Since C30 hopanes do not follow the same trends as other hopanes, it is not advisable to use this class of molecules to reconstruct paleo-pH.

Multiple causes explain the variations in paleo-pH records. Firstly, a comparison of existing paleo-pH records shows that catchment lithology, particularly the presence of carbonate, likely strongly influences pH variations. Secondly, changes in vegetation can explain some of the variations in paleo-pH records. Catchment lithology and vegetation changes can be constrained by literature data and additional analyses such as pollen. Variations in pH values can then be interpreted in terms of the balance between precipitation and evapotranspiration.

Future culturing and laboratory experiments should help confirming the potential occurrence of αβ hopanes in bacteria or other types of living (micro)organisms, or their potential formation during microbial adaptation to changing environment and/or biodegradation of organic matter. Additionally, new sets of data (both paleo-records and modern data) should improve the pH calibrations based on hopane and brGDGT distributions and their potential as paleoenvironmental and paleoclimatic proxies.

Acknowledgments

This work was funded by the ANR project TAPIOCA (ANR-18-CE01-0005) granted to G.Ménot and by a PhD scholarship from the ENS de Lyon to V. Schaaff. Radiocarbon dating has been supported through the French CNRS-INSU-IRD Radiocarbon program and performed at the LMC14 laboratory with the ARTEMIS facility in Saclay. We thank P.Schaeffer for constructive comments on an earlier draft of the manuscript. We thank G. Inglis, D. Naafs and an anonymous reviewer for fruitful reviews. We thank B. Hamelin for his participation to the field work as well as his interactions within the project. We thank S. Ansanay-Alex, I. Antheaume and B. Eddhif for laboratory assistance. This work was carried out within the frame of the LMI DYCOFAC and the CALAKÉ project supported by the Labex OT-Med. We thank IRD Cameroon for its logistic support.

Data availability

Data are available on Pangaea (https://doi.org/10.1594/PANGAEA.963887).

Appendix A. Supplementary Material

Supplementary material includes compound structures (Fig. S.1), complements on hopane analyses (uncertainty measurements) and an annotated HPLC-APCI-MS chromatrogram (Fig. S.2), additional tables and figures on relative abundances and concentrations of brGDGTs and hopanes (Table S.1 and figure S.3) and C_{31} 22S/(22S + 22R) (Fig. S.4). It also includes additional correlations that were tested for this study and comparison with global peat database (Fig. S.5 to S.8) as well as a figure presenting the isotopic composition difference between C_{31} ββ and αβ hopanes (Fig. S.9).

References

Andersen, R., Chapman, S.J., Artz, R.R.E., 2013. Microbial communities in natural and disturbed peatlands: A review. Soil Biol. Biochem. 57, 979–994.

Ausec, L., Kraigher, B., Mandic-Mulec, I., 2009. Differences in the activity and bacterial community structure of drained grassland and forest peat soils. Soil Biol. Biochem. 41, 1874–1881.

Belyea, L.R., Malmer, N., 2004. Carbon sequestration in peatland: patterns and mechanisms of response to climate change. Glob. Change Biol. 10, 1043–1052.

Cao, M., Rueda, G., Rivas-Ruiz, P., Trapote, M.C., Henriksen, M., Vegas-Vilarrúbia, T., Rosell-Melé, A., 2018. Branched GDGT variability in sediments and soils from catchments with marked temperature seasonality. Org. Geochem. 122, 98–114.

Castañeda, I.S., Schouten, S., 2011. A review of molecular organic proxies for examining modern and ancient lacustrine environments. Quat. Sci. Rev. 30, 2851–2891.

Chen, Y., Zheng, F., Yang, H., Yang, W., Wu, R., Liu, X., Liang, H., Chen, H., Pei, H., Zhang, C., Pancost, R.D., Zeng, Z., 2022. The production of diverse brGDGTs by an Acidobacterium providing a physiological basis for paleoclimate proxies. Geochim. Cosmochim. Acta 337, 155–165.

Clymo, R.S., 1963. Ion Exchange in Sphagnum and its Relation to Bog Ecology. Ann. Bot. 27, 309–324.

Clymo, R.S., 1984. The limits to peat bog growth. Philos. Trans. R. Soc. Lond. B Biol. Sci. 303, 605–654.

De Jonge, C., Hopmans, E.C., Zell, C.I., Kim, J.-H., Schouten, S., Sinninghe Damsté, J.S., 2014. Occurrence and abundance of 6-methyl branched glycerol dialkyl glycerol tetraethers in soils: Implications for palaeoclimate reconstruction. Geochim. Cosmochim. Acta 141, 97–112.

De Jonge, C., Kuramae, E.E., Radujković, D., Weedon, J.T., Janssens, I.A., Peterse, F., 2021. The influence of soil chemistry on branched tetraether lipids in mid- and high latitude soils: Implications for brGDGT- based paleothermometry. Geochim. Cosmochim. Acta 310, 95–112.

Dearing Crampton-Flood, E., Tierney, J.E., Peterse, F., Kirkels, F.M.S.A., Sinninghe Damsté, J.S., 2020. BayMBT: A Bayesian calibration model for branched glycerol dialkyl glycerol tetraethers in soils and peats. Geochim. Cosmochim. Acta 268, 142–159.

Dehmer, J., 1995. Petrological and organic geochemical investigation of recent peats with known environments of deposition. Int. J. Coal Geol. 28, 111–138.

Dunfield, P., knowles, R., Dumont, R., Moore, T.R., 1993. Methane production and consumption in

temperate and subarctic peat soils: Response to temperature and pH. Soil Biol. Biochem. 25, 321–326.
Ensminger, A., Van Dorsselaer, A., Spyckerelle, C., Albrecht, P., Ourisson, G., 1974. Pentacyclic triterpenes of the hopane type as ubiquitous geochemical markers: origin and significance. Adv. Org. Geochem. 1973 245–260.
Farrimond, P., Bevan, J.C., Bishop, A.N., 1996. Hopanoid hydrocarbon maturation by an igneous intrusion. Org. Geochem. 25, 149–164.
Farrimond, P., Flanagan, R.L., 1996. Lipid stratigraphy of a Flandrian peat bed (Northumberland, UK): comparison with the pollen record. The Holocene 6, 69–74.
Farrimond, P., Love, G.D., Bishop, A.N., Innes, H.E., Watson, D.F., Snape, C.E., 2003. Evidence for the rapid incorporation of hopanoids into kerogen. Geochim. Cosmochim. Acta 67, 1383–1394.
Fisk, M.C., Ruether, K.F., Yavitt, J.B., 2003. Microbial activity and functional composition among northern peatland ecosystems. Soil Biol. Biochem. 35, 591–602.
Girkin, N.T., Lopes dos Santos, R.A., Vane, C., Ostle, N., Turner, B.L., Sjögersten, S., 2020. Peat properties, dominant vegetation type and microbial community structure in a tropical peatland. Wetlands 40, 1367–1377.
Halamka, T.A., McFarlin, J.M., Younkin, A.D., Depoy, J., Dildar, N., Kopf, S.H., 2021. Oxygen limitation can trigger the production of branched GDGTs in culture. Geochem. Perspect. Lett. 19, 36–39.
Halamka, T.A., Raberg, J.H., McFarlin, J.M., Younkin, A.D., Mulligan, C., Liu, X.-L., Kopf, S.H., 2023. Production of diverse brGDGTs by Acidobacterium Solibacter usitatus in response to temperature, pH, and O2 provides a culturing perspective on brGDGT proxies and biosynthesis. Geobiology 21, 102–118.
Harris, I., Jones, P.D., Osborn, T.J., Lister, D.H., 2014. Updated high-resolution grids of monthly climatic observations–the CRU TS3. 10 Dataset. Int. J. Climatol. 34, 623–642.
Hayes, J.M., Freeman, K.H., Popp, B.N., Hoham, C.H., 1990. Compound-specific isotopic analyses: A novel tool for reconstruction of ancient biogeochemical processes. Proc. 14th Int. Meet. Org. Geochem. 16, 1115–1128.
He, Y., Zhao, C., Zheng, Z., Liu, Z., Wang, N., Li, J., Cheddadi, R., 2015. Peatland evolution and associated environmental changes in central China over the past 40,000 years. Quat. Res. 84, 255–261.
Heipieper, H.J., Neumann, G., Kabelitz, N., Kastner, M., Richnow, H.H., 2004. Carbon isotope fractionation during cis–trans isomerization of unsaturated fatty acids in Pseudomonas putida. Appl. Microbiol. Biotechnol. 66, 285–290.
Hightower, J.W., Hall, W.K., 1967. Tracer Studies of Acid-Catalyzed Reactions. VI. Deuterium Redistribution and Isotope Effects in n-butene Isomerization over Alumina and Silica-Alumina Catalysts. J. Am. Chem. Soc. 89, 778–787.
Hopmans, E.C., Schouten, S., Damsté, J.S.S., 2016. The effect of improved chromatography on GDGT-based palaeoproxies. Org. Geochem. 93, 1–6.
Huang, X., Meyers, P.A., Xue, J., Gong, L., Wang, X., Xie, S., 2015. Environmental factors affecting the low temperature isomerization of homohopanes in acidic peat deposits, central China. Geochim. Cosmochim. Acta 154, 212–228.
Huang, X., Pancost, R.D., Xue, J., Gu, Y., Evershed, R.P., Xie, S., 2018. Response of carbon cycle to drier conditions in the mid-Holocene in central China. Nat. Commun. 9, 1369.
Hughen, K.A., Eglinton, T.I., Xu, L., Makou, M., 2004. Abrupt Tropical Vegetation Response to Rapid Climate Changes. Science 304, 1955–1959.
Huguet, A., Fosse, C., Laggoun-Défarge, F., Toussaint, M.-L., Derenne, S., 2010. Occurrence and distribution of glycerol dialkyl glycerol tetraethers in a French peat bog. Org. Geochem. 41, 559–572.
Huguet, A., Francez, A.-J., Jusselme, M.D., Fosse, C., Derenne, S., 2014. A climatic chamber experiment to test the short term effect of increasing temperature on branched GDGT distribution in Sphagnum peat. Org. Geochem. 73, 109–112.
Huguet, C., Hopmans, E.C., Febo-Ayala, W., Thompson, D.H., Sinninghe Damsté, J.S., Schouten, S., 2006. An improved method to determine the absolute abundance of glycerol dibiphytanyl glycerol

tetraether lipids. Org. Geochem. 37, 1036–1041.
Inglis, G.N., Collinson, M.E., Riegel, W., Wilde, V., Robson, B.E., Lenz, O.K., Pancost, R.D., 2015. Ecological and biogeochemical change in an early Paleogene peat-forming environment: Linking biomarkers and palynology. Palaeogeogr. Palaeoclimatol. Palaeoecol. 438, 245–255.
Inglis, G.N., Naafs, B.D.A., Zheng, Y., McClymont, E.L., Evershed, R.P., Pancost, R.D., 2018. Distributions of geohopanoids in peat: Implications for the use of hopanoid-based proxies in natural archives. Geochim. Cosmochim. Acta 224, 249–261.
Inglis, G.N., Naafs, B.D.A., Zheng, Y., Schellekens, J., Pancost, R.D., "the T-GRES peat database collaborators," 2019. ^{13}C values of bacterial hopanoids and leaf waxes as tracers for methanotrophy in peatlands. Geochim. Cosmochim. Acta 260, 244–256.
Inglis, G.N., Toney, J.L., Zhu, J., Poulsen, C.J., Röhl, U., Jamieson, S.S.R., Pross, J., Cramwinckel, M.J., Krishnan, S., Pagani, M., Bijl, P.K., Bendle, J., 2022. Enhanced Terrestrial Carbon Export From East Antarctica During the Early Eocene. Paleoceanogr. Paleoclimatology 37, e2021PA004348.
Innes, H.E., Bishop, A.N., Head, I.M., Farrimond, P., 1997. Preservation and diagenesis of hopanoids in Recent lacustrine sediments of Priest Pot, England. Role Bact. Process. Sourc. Sediment. Org. Matter 26, 565–576.
Jackson, C.R., Liew, K.C., Yule, C.M., 2009. Structural and Functional Changes with Depth in Microbial Communities in a Tropical Malaysian Peat Swamp Forest. Microb. Ecol. 57, 402–412.
Kluber, L.A., Johnston, E.R., Allen, S.A., Hendershot, J.N., Hanson, P.J., Schadt, C.W., 2020. Constraints on microbial communities, decomposition and methane production in deep peat deposits. PloS One 15, e0223744.
Leifeld, J., Menichetti, L., 2018. The underappreciated potential of peatlands in global climate change mitigation strategies. Nat. Commun. 9, 1071.
Letouzey, R., 1958. Phytogéographie camerounaise. In: Atlas du Cameroun. IRCAM, Yaoundé, p. 6.
Liang, J., Russell, J.M., Xie, H., Lupien, R.L., Si, G., Wang, J., Hou, J., Zhang, G., 2019. Vegetation effects on temperature calibrations of branched glycerol dialkyl glycerol tetraether (brGDGTs) in soils. Org. Geochem. 127, 1–11.
Loisel, J., Gallego-Sala, A.V., Amesbury, M.J., Magnan, G., Anshari, G., Beilman, D.W., Benavides, J.C., Blewett, J., Camill, P., Charman, D.J., Chawchai, S., Hedgpeth, A., Kleinen, T., Korhola, A., Large, D., Mansilla, C.A., Müller, J., van Bellen, S., West, J.B., Yu, Z., Bubier, J.L., Garneau, M., Moore, T., Sannel, A.B.K., Page, S., Väliranta, M., Bechtold, M., Brovkin, V., Cole, L.E.S., Chanton, J.P., Christensen, T.R., Davies, M.A., De Vleeschouwer, F., Finkelstein, S.A., Frolking, S., Gałka, M., Gandois, L., Girkin, N., Harris, L.I., Heinemeyer, A., Hoyt, A.M., Jones, M.C., Joos, F., Juutinen, S., Kaiser, K., Lacourse, T., Lamentowicz, M., Larmola, T., Leifeld, J., Lohila, A., Milner, A.M., Minkkinen, K., Moss, P., Naafs, B.D.A., Nichols, J., O'Donnell, J., Payne, R., Philben, M., Piilo, S., Quillet, A., Ratnayake, A.S., Roland, T.P., Sjögersten, S., Sonnentag, O., Swindles, G.T., Swinnen, W., Talbot, J., Treat, C., Valach, A.C., Wu, J., 2021. Expert assessment of future vulnerability of the global peatland carbon sink. Nat. Clim. Change 11, 70–77.
Loomis, S.E., Russell, J.M., Heureux, A.M., D'Andrea, W.J., Sinninghe Damsté, J.S., 2014. Seasonal variability of branched glycerol dialkyl glycerol tetraethers (brGDGTs) in a temperate lake system. Geochim. Cosmochim. Acta 144, 173–187.
Loomis, S.E., Russell, J.M., Ladd, B., Street-Perrott, F.A., Sinninghe Damsté, J.S., 2012. Calibration and application of the branched GDGT temperature proxy on East African lake sediments. Earth Planet. Sci. Lett. 357, 277–288.
Mackenzie, A.S., McKenzie, D., 1983. Isomerization and aromatization of hydrocarbons in sedimentary basins formed by extension. Geol. Mag. 120, 417–470.
Mackenzie, A.S., Patience, R.L., Maxwell, J.R., Vandenbroucke, M., Durand, B., 1980. Molecular parameters of maturation in the Toarcian shales, Paris Basin, France—I. Changes in the configurations of acyclic isoprenoid alkanes, steranes and triterpanes. Geochim. Cosmochim. Acta 44, 1709–1721.
Martínez-Sosa, P., Tierney, J.E., Stefanescu, I.C., Dearing Crampton-Flood, E., Shuman, B.N., Routson, C., 2021. A global Bayesian temperature calibration for lacustrine brGDGTs. Geochim. Cosmochim.

Acta 305, 87–105.
Marwanto, S., Watanabe, T., Iskandar, W., Sabiham, S., Funakawa, S., 2018. Effects of seasonal rainfall and water table movement on the soil solution composition of tropical peatland. Soil Sci. Plant Nutr. 64, 386–395.
McClymont, E.L., Mauquoy, D., Yeloff, D., Broekens, P., Van Geel, B., Charman, D.J., Pancost, R.D., Chambers, F.M., Evershed, R.P., 2008. The disappearance of Sphagnum imbricatum from Butterburn Flow, UK. The Holocene 18, 991–1002.
Miller, D.R., Habicht, M.H., Keisling, B.A., Castañeda, I.S., Bradley, R.S., 2018. A 900-year New England temperature reconstruction from in situ seasonally produced branched glycerol dialkyl glycerol tetraethers (brGDGTs). Clim. Past 14, 1653–1667.
Moore, P.D., 1989. The ecology of peat-forming processes: a review. Int. J. Coal Geol. 12, 89–103.
Naafs, B.D.A., Inglis, G., Blewett, J., McClymont, E.L., Lauretano, V., Xie, S., Evershed, R., Pancost, R., 2019. The potential of biomarker proxies to trace climate, vegetation, and biogeochemical processes in peat: A review. Glob. Planet. Change 179, 57–79.
Naafs, B.D.A., Inglis, G.N., Zheng, Y., Amesbury, M.J., Biester, H., Bindler, R., Blewett, J., Burrows, M.A., Del Castillo Torres, D., Chambers, F.M., 2017. Introducing global peat-specific temperature and pH calibrations based on brGDGT bacterial lipids. Geochim. Cosmochim. Acta 208, 285–301.
Naafs, B.D.A., Oliveira, A.S.F., Mulholland, A.J., 2021. Molecular dynamics simulations support the hypothesis that the brGDGT paleothermometer is based on homeoviscous adaptation. Geochim. Cosmochim. Acta 312, 44–56.
Nichols, J.E., Peteet, D.M., Moy, C.M., Castañeda, I.S., McGeachy, A., Perez, M., 2014. Impacts of climate and vegetation change on carbon accumulation in a south-central Alaskan peatland assessed with novel organic geochemical techniques. The Holocene 24, 1146–1155.
O'Leary, M.H., 1980. [4] Determination of heavy-aton isotope effects on enzyme-catalyzed reactions. In: Purich, D.L. (Ed.), Methods in Enzymology. Academic Press, pp. 83–104.
Ourisson, G., Rohmer, M., Poralla, K., 1987. Prokaryotic Hopanoids and other Polyterpenoid Sterol Surrogates. Annu. Rev. Microbiol. 41, 301–333.
Pan, H., Culp, R.A., Noakes, J.E., Sun, M.-Y., 2014. Effects of growth stages, respiration, and microbial degradation of phytoplankton on cellular lipids and their compound-specific stable carbon isotopic compositions. J. Exp. Mar. Biol. Ecol. 461, 7–19.
Pancost, R.D., Baas, M., van Geel, B., Sinninghe Damsté, J.S., 2003. Response of an ombrotrophic bog to a regional climate event revealed by macrofossil, molecular and carbon isotopic data. The Holocene 13, 921–932.
Pancost, R.D., Damsté, J.S.S., 2003. Carbon isotopic compositions of prokaryotic lipids as tracers of carbon cycling in diverse settings. Chem. Geol. 195, 29–58.
Pancost, R.D., Steart, D.S., Handley, L., Collinson, M.E., Hooker, J.J., Scott, A.C., Grassineau, N.V., Glasspool, I.J., 2007. Increased terrestrial methane cycling at the Palaeocene–Eocene thermal maximum. Nature 449, 332–335.
Pancost, R.D., van Geel, B., Baas, M., Damsté, J.S.S., 2000. δ13C values and radiocarbon dates of microbial biomarkers as tracers for carbon recycling in peat deposits. Geology 28, 663–666.
Pearson, A., Flood Page, S.R., Jorgenson, T.L., Fischer, W.W., Higgins, M.B., 2007. Novel hopanoid cyclases from the environment. Environ. Microbiol. 9, 2175–2188.
Peiseler, B., Rohmer, M., 1992. Prokaryotic triterpenoids of the hopane series. Bacteriohopanetetrols of new side-chain configuration from Acetobacter species. J. Chem. Res. Synop. Print 298–299.
Pérez-Angel, L.C., Sepúlveda, J., Molnar, P., Montes, C., Rajagopalan, B., Snell, K., Gonzalez-Arango, C., Dildar, N., 2020. Soil and Air Temperature Calibrations Using Branched GDGTs for the Tropical Andes of Colombia: Toward a Pan-Tropical Calibration. Geochem. Geophys. Geosystems 21, e2020GC008941.
Peters, K.E., Moldowan, J.M., McCaffrey, M.A., Fago, F.J., 1996. Selective biodegradation of extended hopanes to 25-norhopanes in petroleum reservoirs. Insights from molecular mechanics. Org. Geochem. 24, 765–783.
Peterse, F., van der Meer, J., Schouten, S., Weijers, J.W.H., Fierer, N., Jackson, R.B., Kim, J.-H.,

Sinninghe Damsté, J.S., 2012. Revised calibration of the MBT–CBT paleotemperature proxy based on branched tetraether membrane lipids in surface soils. Geochim. Cosmochim. Acta 96, 215–229.
Quirk, M.M., Wardroper, A.M.K., Wheatley, R.E., Maxwell, J.R., 1984. Extended hopanoids in peat environments. Chem. Geol. 42, 25–43.
Requejo, A.G., Halpern, H.I., 1989. An unusual hopane biodegradation sequence in tar sands from the Pt Arena (Monterey) Formation. Nature 342, 670–673.
Ries-Kautt, M., Albrecht, P., 1989. Hopane-derived triterpenoids in soils. Chem. Geol. 76, 143–151.
Rohmer, M., Bouvier-Nave, P., Ourisson, G., 1984. Distribution of Hopanoid Triterpenes in Prokaryotes. Microbiology.
Rosa-Putra, S., Nalin, R., Domenach, A.-M., Rohmer, M., 2001. Novel hopanoids from Frankia spp. and related soil bacteria. Eur. J. Biochem. 268, 4300–4306.
Russell, N.J., Fukunaga, N., 1990. A comparison of thermal adaptation of membrane lipids in psychrophilic and thermophilic bacteria. FEMS Microbiol. Lett. 75, 171–182.
Sáenz, J.P., Grosser, D., Bradley, A.S., Lagny, T.J., Lavrynenko, O., Broda, M., Simons, K., 2015. Hopanoids as functional analogues of cholesterol in bacterial membranes. Proc. Natl. Acad. Sci. 112, 11971–11976.
Schaaff, V., Sebag, D., Makou, M., Grossi, V., Antheaume, I., Hamelin, B., Garcin, Y., Ngounou Ngatcha, B., Deschamps, P., Ménot, G., 2023. Modeling the decomposition signal and correcting bulk organic data from a peat deposit, a case study at low latitudes (Cameroon). Org. Geochem. 179, 104589.
Schmerk, C.L., Bernards, M.A., Valvano, M.A., 2011. Hopanoid production is required for low-pH tolerance, antimicrobial resistance, and motility in Burkholderia cenocepacia. J. Bacteriol. 193, 6712–6723.
Schouten, S., Hoefs, M.J.L., Sinninghe Damsté, J.S., 2000a. A molecular and stable carbon isotopic study of lipids in late Quaternary sediments from the Arabian Sea. Org. Geochem. 31, 509–521.
Schouten, S., Hopmans, E.C., Damsté, J.S.S., 2013. The organic geochemistry of glycerol dialkyl glycerol tetraether lipids: A review. Org. Geochem. 54, 19–61.
Schouten, S., Hopmans, E.C., Pancost, R.D., Damsté, J.S.S., 2000b. Widespread occurrence of structurally diverse tetraether membrane lipids: Evidence for the ubiquitous presence of low-temperature relatives of hyperthermophiles. Proc. Natl. Acad. Sci. 97, 14421–14426.
Schwartz-Narbonne, R., Schaeffer, P., Lengger, S.K., Blewett, J., Martin Jones, D., Motsch, E., Crombie, A., Jetten, M.S.-M., Mikkelsen, D., Normand, P., Nuijten, G.H.L., Pancost, R.D., Rush, D., 2023. Bacterial physiology highlighted by the δ13C fractionation of bacteriohopanetetrol isomers. Org. Geochem. 181, 104617.
Sinninghe Damsté, J.S., Hopmans, E.C., Pancost, R.D., Schouten, S., Geenevasen, J.A., 2000. Newly discovered non-isoprenoid glycerol dialkyl glycerol tetraether lipids in sediments. Chem. Commun. 1683–1684.
Sinninghe Damsté, J.S., Rijpstra, W.I.C., Foesel, B.U., Huber, K.J., Overmann, J., Nakagawa, S., Kim, J.J., Dunfield, P.F., Dedysh, S.N., Villanueva, L., 2018. An overview of the occurrence of ether- and ester-linked iso-diabolic acid membrane lipids in microbial cultures of the Acidobacteria: Implications for brGDGT paleoproxies for temperature and pH. Org. Geochem. 124, 63–76.
Sinninghe Damsté, J.S., Rijpstra, W.I.C., Hopmans, E.C., Foesel, B.U., Wüst, P.K., Overmann, J., Tank, M., Bryant, D.A., Dunfield, P.F., Houghton, K., Stott, M.B., 2014. Ether- and Ester-Bound iso-Diabolic Acid and Other Lipids in Members of Acidobacteria Subdivision 4. Appl. Environ. Microbiol. 80, 5207–5218.
Sinninghe Damsté, J.S., Rijpstra, W.I.C., Hopmans, E.C., Weijers, J.W.H., Foesel, B.U., Overmann, J., Dedysh, S.N., 2011. 13,16-Dimethyl Octacosanedioic Acid (iso-Diabolic Acid), a Common Membrane-Spanning Lipid of Acidobacteria Subdivisions 1 and 3. Appl. Environ. Microbiol. 77, 4147–4154.
Sinninghe Damsté, J.S., Van Duin, A.C.T., Hollander, D., Kohnen, M.E.L., De Leeuw, J.W., 1995. Early diagenesis of bacteriohopanepolyol derivatives: Formation of fossil homohopanoids. Geochim. Cosmochim. Acta 59, 5141–5157.
Smittenberg, R.H., Pancost, R.D., Hopmans, E.C., Paetzel, M., Sinninghe Damsté, J.S., 2004. A 400-

year record of environmental change in an euxinic fjord as revealed by the sedimentary biomarker record. Palaeogeogr. Palaeoclimatol. Palaeoecol. 202, 331–351.
Sun, M.-Y., Zou, L., Dai, J., Ding, H., Culp, R.A., Scranton, M.I., 2004. Molecular carbon isotopic fractionation of algal lipids during decomposition in natural oxic and anoxic seawaters. Org. Geochem. 35, 895–908.
Sun, Q., Chu, G., Liu, M., Xie, M., Li, S., Ling, Y., Wang, X., Shi, L., Jia, G., Lü, H., 2011. Distributions and temperature dependence of branched glycerol dialkyl glycerol tetraethers in recent lacustrine sediments from China and Nepal. J. Geophys. Res. Biogeosciences 116.
Swanson, D.K., Grigal, D.F., 1991. Biomass, structure, and trophic environment of peatland vegetation in Minnesota. Wetlands 11, 279–302.
Talbot, H.M., McClymont, E.L., Inglis, G.N., Evershed, R.P., Pancost, R.D., 2016. Origin and preservation of bacteriohopanepolyol signatures in Sphagnum peat from Bissendorfer Moor (Germany). Org. Geochem. 97, 95–110.
Too, C.C., Keller, A., Sickel, W., Lee, S.M., Yule, C.M., 2018. Microbial community structure in a Malaysian tropical peat swamp forest: the influence of tree species and depth. Front. Microbiol. 9, 2859.
Tripathi, B.M., Song, W., Slik, J.W.F., Sukri, R.S., Jaafar, S., Dong, K., Adams, J.M., 2016. Distinctive Tropical Forest Variants Have Unique Soil Microbial Communities, But Not Always Low Microbial Diversity. Front. Microbiol. 7.
Vinçon-Laugier, A., Cravo-Laureau, C., Mitteau, I., Grossi, V., 2017. Temperature-Dependent Alkyl Glycerol Ether Lipid Composition of Mesophilic and Thermophilic Sulfate-Reducing Bacteria. Front. Microbiol. 8.
Waldrop, M.P., Firestone, M.K., 2006. Response of Microbial Community Composition and Function to Soil Climate Change. Microb. Ecol. 52, 716–724.
Wang, M., Zheng, Z., Man, M., Hu, J., Gao, Q., 2017. Branched GDGT-based paleotemperature reconstruction of the last 30,000years in humid monsoon region of Southeast China. Chem. Geol. 463, 94–102.
Webb, T., 1986. Is vegetation in equilibrium with climate? How to interpret late-Quaternary pollen data. Vegetatio 67, 75–91.
Weber, Y., Sinninghe Damsté, J.S., Zopfi, J., De Jonge, C., Gilli, A., Schubert, C.J., Lepori, F., Lehmann, M.F., Niemann, H., 2018. Redox-dependent niche differentiation provides evidence for multiple bacterial sources of glycerol tetraether lipids in lakes. Proc. Natl. Acad. Sci. 115, 10926–10931.
Weijers, J.W., Schouten, S., Hopmans, E.C., Geenevasen, J.A., David, O.R., Coleman, J.M., Pancost, R.D., Sinninghe Damsté, J.S., 2006. Membrane lipids of mesophilic anaerobic bacteria thriving in peats have typical archaeal traits. Environ. Microbiol. 8, 648–657.
Weijers, J.W.H., Panoto, E., van Bleijswijk, J., Schouten, S., Rijpstra, W.I.C., Balk, M., Stams, A.J.M., Damsté, J.S.S., 2009. Constraints on the Biological Source(s) of the Orphan Branched Tetraether Membrane Lipids. Geomicrobiol. J. 26, 402–414.
Weijers, J.W.H., Schouten, S., van den Donker, J.C., Hopmans, E.C., Sinninghe Damsté, J.S., 2007. Environmental controls on bacterial tetraether membrane lipid distribution in soils. Geochim. Cosmochim. Acta 71, 703–713.
Weijers, J.W.H., Steinmann, P., Hopmans, E.C., Schouten, S., Sinninghe Damsté, J.S., 2011. Bacterial tetraether membrane lipids in peat and coal: Testing the MBT–CBT temperature proxy for climate reconstruction. Org. Geochem. 42, 477–486.
Welander, P.V., Coleman, M.L., Sessions, A.L., Summons, R.E., Newman, D.K., 2010. Identification of a methylase required for 2-methylhopanoid production and implications for the interpretation of sedimentary hopanes. Proc. Natl. Acad. Sci. 107, 8537–8542.
Welander, P.V., Hunter, R.C., Zhang, L., Sessions, A.L., Summons, R.E., Newman, D.K., 2009. Hopanoids Play a Role in Membrane Integrity and pH Homeostasis in *Rhodopseudomonas palustris* TIE-1. J. Bacteriol. 191, 6145–6156.
Williams, R.T., Crawford, R.L., 1983. Microbial diversity of Minnesota peatlands. Microb. Ecol. 9, 201–214.

Winsborough, C., Basiliko, N., 2010. Fungal and Bacterial Activity in Northern Peatlands. Geomicrobiol. J. 27, 315–320.
Xie, S., Nott, C.J., Avsejs, L.A., Maddy, D., Chambers, F.M., Evershed, R.P., 2004. Molecular and isotopic stratigraphy in an ombrotrophic mire for paleoclimate reconstruction. Geochim. Cosmochim. Acta 68, 2849–2862.
Zhang, L., Wu, Z., Chen, J., Liu, D., Chen, P., 2022. Spatiotemporal patterns and drivers of net primary production in the terrestrial ecosystem of the Dajiuhu Basin, China, between 1990 and 2018. Ecol. Inform. 72, 101839.
Zhang, Y., Huang, X., Wang, R., Naafs, B.D.A., 2020. The distribution of long-chain n-alkan-2-ones in peat can be used to infer past changes in pH. Chem. Geol. 544, 119622.
Zheng, Y., Li, Q., Wang, Z., Naafs, B.D.A., Yu, X., Pancost, R.D., 2015. Peatland GDGT records of Holocene climatic and biogeochemical responses to the Asian Monsoon. Org. Geochem. 87, 86–95.